Progress in Oceanography 237 (2025) 103525

Contents lists available at ScienceDirect

Progress in Oceanography

journal homepage: www.elsevier.com/locate/pocean

A time series of water mass transports through the Balearic Channels using an ocean circulation inverse method: 1996–2022

Manuel Vargas-Yáñez [a,*], Maxandre Ouradou [b], Francina Moya [a], Enrique Ballesteros [a], Cristina Alonso [a], Mariano Serra [c], Safo Piñeiro [c], Vicenç Moltó [c], Rocío Santiago [c], Rosa Balbín [c], Silvia Sánchez-Aguado [c], Mª Carmen García-Martínez [c], Gabriel Jordà [c], Alonso Hernández-Guerra [d]

[a] Instituto Español de Oceanografía, Consejo Superior de Investigaciones Científicas (IEO-CSI). Centro Oceanográfico de Málaga, Puerto pesquero de Fuengirola 29640 Fuengirola (Málaga), Spain

[b] Ecole Nationale de Meteorologie, Toulouse, France

[c] Instituto Español de Oceanografía, Consejo Superior de Investigaciones Científicas (IEO-CSI). Centro Oceanográfico de Baleares, Muelle de Poniente, 07015 Palma, Spain

[d] Instituto de Oceanografía y Cambio Global (IOCAG), Universidad de Las Palmas de Gran Canaria (ULPGC), Spain

A R T I C L E I N F O

Keywords:
Ibiza channel
Mallorca channel
Balearic channels
Inverse modelling
North Balearic current
Western mediterranean

A B S T R A C T

Time series of temperature and salinity from CTD (Conductivity Temperature Depth) sections in the Ibiza and Mallorca Channels from 1996 to 2022 are used to calculate a time series of transports of Atlantic Water (AW), Western Intermediate Water (WIW), Levantine Intermediate Water (LIW) and Western Mediterranean Deep Water (WMDW). The oceanographic stations were distributed on two triangular closed boxes for the application of inverse circulation modelling. A data set of 80 oceanographic campaigns was initially considered. After examination and interpolation of the data, only 23 campaigns contained the complete sections forming the two boxes and were suitable for the calculation of transports using the inverse method. Over the course of 42 oceanographic cruises, only the southern sections of the Ibiza and Mallorca Channels were completed. In these cases, transports were derived from geostrophic velocities, using the sea floor as a reference level of no motion, and without employing the inverse method. The results from both methodologies showed a prevailing southward annual transport of the upper layer (AW + WIW) ranging between −0.1 Sv and −0.21 Sv in the Ibiza Channel and a northward transport between 0.07 Sv and 0.09 Sv in the Mallorca Channel (depending on the methodology used). A subjective classification of the circulation patterns for each individual campaign revealed the existence of 5 circulation modes: Northern Current mode, inflow mode, two-way circulation, reversed two-way circulation, and eddy circulation mode. The two-way circulation mode, with a southward flow at the western side of both channels and a northward flow at the eastern sides, was the most frequently observed circulation pattern. However, the inter-annual variability seems to be larger than the seasonal signal and it was very difficult to establish a seasonality in the occurrence of these circulation modes. LIW flows to the south in the Ibiza Channel and to the north in the Mallorca one, but the transports of this water mass were very low, suggesting that the main path of LIW follows the northern slope of the Islands, within the North Balearic Current. These results are used to speculate about the circulation and mass budget in the Northwestern Mediterranean.

1. Introduction

The circulation of the Western Mediterranean (WMED), as well as that of the Eastern Mediterranean (EMED), is forced by the fresh water deficit and the net heat loss of both basins (Schroeder et al., 2023). This forcing is responsible for an inflow of Atlantic Water (AW) through the Strait of Gibraltar (∼1 Sv) that crosses the WMED until the Sicily Channel where it flows into the EMED. In a very simplistic way, it could be considered that the circulation of the AW within the WMED is made of two main elements. The first is the Atlantic Current, which crosses the

* Corresponding author.
E-mail address: manolo.vargas@ieo.csic.es (M. Vargas-Yáñez).

https://doi.org/10.1016/j.pocean.2025.103525
Received 22 January 2024; Received in revised form 11 June 2025; Accepted 11 June 2025
Available online 13 June 2025

Alboran Sea and then flows through the Algerian Basin (as the Algerian Current) towards the Sicily Channel. This first structure frequently includes two anticyclonic gyres in the Alboran Sea (Brett et al., 2020; Viúdez and Tintoré, 1995): one in the Western Alboran sub-basin and a second one in the Eastern sub-basin. In addition, two cyclonic gyres can be found along the Algerian Current: one centered at 37° 30′ N, 2° 30′ E (Western Algerian Gyre; WAG) and a another one centred at 38° 30′ N, 6° 00′ E (Eastern Algerian Gyre; EAG; Mallil et al., 2022; Escudier et al., 2016; Testor et al., 2005). Cyclonic and anticyclonic eddies are frequently generated along the Algerian Current. The anticlyclonic ones are usually deeper and can detach from the main current becoming open sea Algerian Eddies (AEs) that can last from several months to three years (Vargas-Yáñez et al., 2023a; Mallil et al., 2022; Ruiz et al., 2002; Puillat et al., 2002) and drift within the WAG and EAG (Escudier et al., 2016).

The second component of this circulation scheme is a recirculation cell that flows cyclonically around the riparian countries of the WMED (Millot and Taupier-Letage, 2005) until closing the circuit at the Almeria-Oran Front (Troupin et al., 2019; Renault et al., 2012). This latter front would be the result of the meeting of fresh AW recently advected into the Mediterranean Sea through Gibraltar, with AW severely modified after recirculating within the WMED.

The two elements briefly described above are interconnected. On one hand, the WMED has a fresh water deficit in the whole basin, which increases northwards (Schroeder et al., 2023; Boukthir and Barnier, 2000). On the other hand, a fraction of the AW flowing into the Ligurian Sea, the Gulf of Lions and the Catalan-Balearic Sea contributes to the formation of the Western Mediterranean Deep Water (WMDW) and Western Intermediate Water (WIW). Therefore, in a stationary state, the conservation of the volume of AW in the northern WMED (Provencal Basin) requires that the net evaporation and the volumes of AW transformed into deep and intermediate waters be replaced by AW from the Algerian Basin. Besides this, the net heat flux at the sea surface is negative (from the sea to the atmosphere) in the Gulf of Lions and Ligurian Sea, whereas it is positive at the central and southern parts of the WMED (Schroeder et al., 2023; Ruiz et al., 2008). Therefore, the stationary state also requires a net heat transport towards the northernmost sector of the WMED. The heat and freshwater balance of the WMED, together with the cyclonic circulation of this basin implies that fresh and warm water should flow northwards in the eastern branch of the recirculating cyclonic cell, whereas colder and saltier water should flow southwards in the western sector of the WMED. The balance between both flows would be a net volume and heat transport to the north (Bethoux, 1980).

The western branch of this recirculating cyclonic cell would be the southward extension of the Northern Current that flows along the Ligurian Sea and the continental slope in front of the Gulf of Lions. This current mainly alludes to AW, but it also carries LIW and WIW with a volume transport that fluctuates between 0.5 and 2 Sv, depending on the authors. This large variability is linked to the seasonal cycle of this structure, the seasonality associated with the winter convection processes that take place in this region (Béranger et al., 2005; Millot and Taupier-Letage, 2005; Pinot and Garnachaud, 1999; Conan and Millot, 1995)) and the large inter-annual variability of such processes (Margirier et al., 2020; Herrmann et al., 2010).

The southward progression of AW, and also WIW and LIW, is hindered by the presence of the Balearic Islands and Channels which partially deflect the current to the northeast, forming the North Balearic Current (Vargas-Yáñez et al., 2020; Juza et al., 2015; 2013). These channels have been described as a choke point for the water exchange between the Provencal and Algerian basins (Vargas-Yáñez et al., 2020; Barceló-Llull et al., 2019; Heslop et al., 2012) and have received an increasing attention since the first works carried out during the beginning of the 1990s decade by López-Jurado and Díaz del Río (1994) and Castellón et al. (1990). However, our knowledge of the circulation and water transports through these channels remains incomplete, despite their paramount importance for the understanding of the circulation of the WMED. The main problems for describing the circulation through the Balearic Channels arise from its high variability at different time scales, including inter-annual, seasonal and high frequency variability, this later linked to an intense mesoscale activity in the channels (Vargas-Yáñez et al., 2020; Barceló-Llull et al., 2019; Juza et al., 2013; Heslop et al., 2012; Pinot et al., 2002). Furthermore, the estimation of seasonal mean values for the transports through the channels is obscured by the fact that mesoscale variability could be larger than the amplitude of the seasonal cycle (Barceló-Llull et al., 2019). This makes necessary the use of time series as long as possible for such calculations. In this regard, Castellón et al. (1990) only used CTD data from two surveys carried out in May-June 1989 and López-Jurado and Díaz del Río (1994) also analysed two surveys carried out in the Ibiza Channel in November 1990 and March 1991. Pinot and Garnachaud (1999) analysed CTD data from one single survey in June 1993 for studying the circulation of the Catalan Sea and the Balearic Channels. The first attempt to analyze a time series of temperature and salinity sections for addressing the seasonal variability of the circulation in the Balearic Channels is due to Pinot et al. (2002). These authors analysed a set of 13 CTD surveys in the Ibiza and Mallorca Channels extending from 1996 to 1998. Juza et al. (2013), Heslop et al. (2012) used a time series of glider data from February to June 2011 for studying the mesoscale activity and the transports through the Ibiza Channel. Barceló-Llull et al. (2019) used a long time series of temperature and salinity glider data, extending from 2011 to 2018 in the Mallorca Channel. These authors studied the long-term mean transports and their seasonal and high frequency variability.

To our knowledge, the longest time series of temperature and salinity data from both the Ibiza and Mallorca Channels are those analysed in Vargas-Yáñez et al. (2021; 2020). These time series extended from 1996 to 2019. However, Vargas-Yáñez et al. (2021) only considered the long-term variability of temperature, salinity and density fields in the Balearic Channels without addressing the calculation of transports through them. Vargas-Yáñez et al. (2020) calculated the mean seasonal transports for AW, WIW, LIW and WMDW, but not the variability superimposed on these climatological cycles. Besides this, the mean seasonal transports were calculated from mean seasonal temperature and salinity fields, and no time series of transports were considered. In the present work, we extend the time series used in these previous works to 2022. In addition, volume and mass transports through the Ibiza and Mallorca Channels are calculated for each single survey from 1996 to 2022. In this way, a 27 years-long time series of transports through the Balearic Channels are calculated using an inverse circulation method. The mean seasonal cycle is calculated averaging the transports for each season of the year, instead of calculating the transports corresponding to the mean seasonal temperature and salinity fields (Vargas-Yáñez et al., 2020). The varibility associated to the inter-annual and higher frequency mesoscale activity is also estimated. Different modes of circulation within the Channels and the frequency of their occurrence are investigated following Barceló-Llull et al. (2019) and Heslop et al. (2012).

The objectives of this work can be summarized as follows:

1. To obtain time series of mass transports through the Balearic Channels for AW, WIW, LIW, and WMDW from 1996 to 2022. To our knowledge, this is the first time a long-term transport time series is presented for both Balearic Channels.
2. To compare average transports obtained from these time series with those derived from averaged temperature-salinity (TS) fields, as done in Vargas-Yáñez et al. (2020).
3. To describe the seasonal variability of mass transports throughout the seasonal cycle, and to compare the amplitude of these cycles with the interannual variability.
4. To identify different circulation modes through the Balearic Channels, and to determine the most likely season for each mode. For this objective, we follow the methodology proposed by Barceló-Llull

(2019), extending the length of the analysed time series and covering both channels.

2. Data and methods

2.1. RADMED project

RADMED (series temporales de datos oceanográficos en el Mediterráneo; Time series of oceanographic data in the Mediterranean) is a project devoted to the multidisciplinary monitoring of the Spanish Mediterranean waters, funded by the Instituto Español de Oceanografía, belonging to the Consejo Superior de Investigaciones Científicas (IEO-CSIC, Spanish Institute of Oceanography, from Spanish National Research Council). This project consists of a set of oceanographic stations covering the continental shelf and slope waters, as well as some deep stations, in the Spanish Mediterranean (see Vargas-Yáñez et al., 2023b; Vargas-Yáñez et al., 2017; López-Jurado et al. 2015 for the positions of the stations and other details). All the stations are visited with a seasonal periodicity (four times per year) and include CTD (Conductivity-Temperature-Depth) casts.

RADMED project started in 2007. Nevertheless, some of its oceanographic stations had been monitored by IEO since the 1990s within the framework of other projects (Vargas-Yáñez et al., 2017). This is the case of the 37 stations covering the Ibiza and Mallorca Channels (Fig. 1). These stations started to be visited approximately quarterly in 1996 in the frame of the Project Canales (Pinot et al., 2002). The stations were distributed in two triangles in order to form two closed boxes for the application of circulation inverse methods (Vargas-Yáñez et al., 2020; Pinot et al., 2002; Pinot and Ganachaud, 1999). Table S1 in supplementary material shows the position and nominal depth for each of the stations within the Balearic Channels.

The total number of campaigns used in the present work is 80, spanning from March 1996 to November 2022. The year and month of each campaign are listed in Table S2 in the supplementary material. Metadata are available in SeaDataNet and data are accessible upon request. They are also freely available at discrete depth levels in IBAMar database http://www.ba.ieo.es/es/ibamar.

2.2. Inverse methods and interpolation

Inverse models were developed by Wunsch (1996; 1978) and thereafter have been widely applied for the calculation of mass, heat and salt transports in different parts of the world oceans (see Hernández-Guerra et al., 2019; Hernández-Guerra et al., 2017; Casanova-Masjoan et al., 2018; Hernández-Guerra and Talley, 2016 for just a few examples). Such models were also applied to the calculation of water mass transports in the Balearic Channels by Vargas-Yáñez et al. (2020), Pinot et al. (2002) and Pinot and Ganachaud (1999). The details concerning this methodology can be consulted in Wunsch (1996; 1978), nevertheless, here we include a brief description for the sake of completeness and a more detailed description is also presented in supplementary material.

If a certain pressure level p_{ref} is considered as the reference one, the geostrophic velocity between a pair of oceanographic stations (CTD casts), relative to the reference level, can be calculated at any pressure level by means of the geostrophic approximation.

$$v(p) = v(p_{ref}) + \left(\frac{\partial \varphi}{\partial x}\right)_p$$

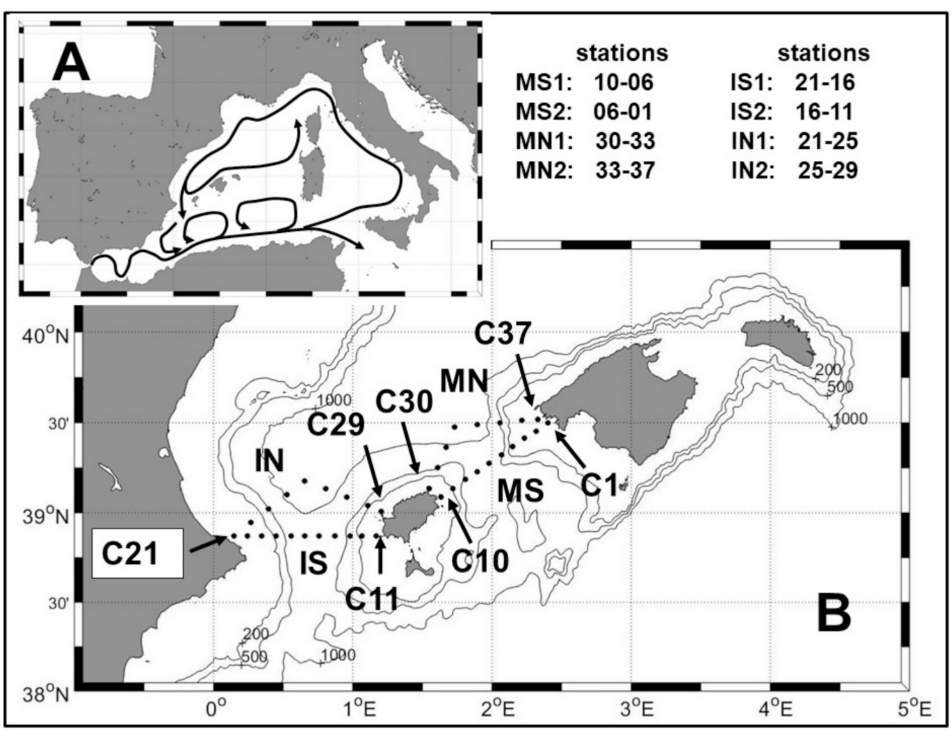

Fig. 1. A. Map of the Western Mediterranean and scheme of its circulation. B. Zoom of the Balearic Islands and Channels and position of RADMED stations forming two triangles in the Mallorca and Ibiza Channels (MN and MS for the Mallorca Channel and IN and IS for the Ibiza Channel). The base of the Mallorca Channel triangle is named Mallorca South section (MS) and is made of the stations C1 to C10. MS section is subdivided into two subsections for the calculation of the transports: MS1 (western part of the section) and MS2 (eastern part of it). Fig. 1 shows the stations used for the calculation of transports corresponding to each subsection. The northern part of the Mallorca Channel is named Mallorca North (MN) and is made of the stations C30 to C37. MN section is subdivided into two subsections (see Fig. 1) for the calculation of the transports: MN1 (western part of the section) and MN2 (eastern part of it). Similarly, the base of the Ibiza Channel triangle is named Ibiza South section (IS) and is made of the stations C11 to C21. IS section is subdivided into two subsections IS1 (western part of the section) and IS2 (eastern part of it) and the northern part of the Ibiza Channel is named Ibiza North (IN) and is made of the stations C21 to C29. Notice that IS and IN share station C21. IN section is subdivided into two subsections: IN1 (western part of the section) and IN2 (eastern part of it).

Being v the velocity normal to the section formed by the two oceanographic stations, x the distance between stations and ϕ the dynamic height of the pressure level p referred to the level p_{ref} defined by:

$\varphi = \int_p^{pref} \alpha dp$ $\alpha = 1/\rho$ is the specific volume and ρ is the sea water density. In practice the specific volume anomaly is used instead.

In order to calculate the geostrophic velocity, it is frequently assumed that the velocity is known at the reference level as it is usually considered a no-motion layer. Obviously, this assumption introduces some degree of uncertainty in the calculations.

However, when oceanographic stations are distributed within a closed box, it is possible to apply inverse circulation methods. In this framework, rather than assuming an arbitrary velocity at the reference level, the velocities are estimated by imposing a set of physical constraints that enable their determination. Following previous applications of inverse modelling in the Balearic Channels, and to facilitate comparison with those studies, the present work adopts a similar approach. Specifically, we impose mass conservation over four distinct layers, as well as over the entire volume enclosed by the box. These layers are defined according to their sigma-theta (σ_θ) ranges ($\sigma_\theta = \rho(\theta, S, p = 0)$-$1000$, where ρ is density, θ is potential temperature, S is salinity, and p is pressure). The Atlantic Water (AW) layer is defined as those waters with sigma theta lower than 28.8 kg/m^3, the Western Intermediate Water (WIW) layer is that with sigma theta between 28.8 kg/m^3 and 29.05 kg/m^3, the Levantine Intermediate Water (LIW) layer is between 29.05 kg/m^3 and 29.1 kg/m^3, and the Western Mediterranean Deep Water (WMDW) layer is made of those waters denser than 29.1 kg/m^3 (see Pinot and Ganachaud, 1999). The mass conservation for each of these layers and for the whole water column was imposed for the calculation of the velocity at the reference level. Once the reference velocity was calculated from the inverse method, the mass transports associated with each water mass were obtained.

The stations from RADMED project corresponding to the Mallorca and Ibiza Channels are arranged in two triangles. Each triangle is made of two sections: a southern straight section, and a broken northern section. The southern and northern sections of both channels were further divided in subsections 1 and 2 in order to provide a more detailed description of the water mass transports at the eastern and western sectors of the channels and for comparison with previous works in which this subdivision was applied (Vargas-Yáñez et al., 2020; Pinot et al., 2002; Pinot and Ganachaud, 1999). Finally, the subsections that will be considered hereafter are named as Mallorca South 1 and 2 (MS1, MS2), Mallorca North 1 and 2 (MN1, MN2), Ibiza South 1 and 2 (IS1, IS2) and Ibiza North 1 and 2 (IN1, IN2). The stations corresponding to each section can be consulted in Fig. 1.

However, during the 80 campaigns analysed in this work, it was very frequent that the sections were not completed, and in some cases, even some complete sections were missed because of bad weather conditions, vessel breakdowns or technical problems with the instrumentation. In other cases, the CTD did not reach the nominal depth of the station or the final temperature and salinity profiles presented some gaps. In order to have a set of complete boxes as long as possible, missing data were interpolated whenever feasible.

Missing data within the upper 10 m of the water column were filled with the available data from the most superficial depth within the upper 10 m, assuming that the upper surface layer has very homogeneous properties because of the stirring caused by waves. Gaps in the upper 100 m of the water column (deeper than 10 m) were filled by means of Optimal Statistical Interpolation. The seasonal background fields used for this interpolation were obtained from the average values estimated from the temperature and salinity time series, and the covariance functions and noise to signal ratios for the temperature and salinity fields were those estimated in Vargas-Yáñez et al. (2020) from the analysis of the time series. Further details about this interpolation methodology can be consulted in Gomis et al., 2001; Pedder, 1993; Thiébaux and Pedder, 1987, for instance. However, we also include a brief description in the supplementary material for the sake of completeness.

Optimal Statistical Interpolation was only applied when at least half of the stations within the section were available and only if these stations included those at the extremes of the sections for avoiding extrapolation. When a CTD profile reached a depth of 600 m or more, but did not reach the nominal depth of the station, the missing data were filled using the closest station.

After interpolation, 23 complete campaigns were available (see columns 1 and 2 in Table 1 for the year and month of such campaigns). Besides these complete campaigns, there were others for which southern sections (straight sections) of both Channels were completed, but the northern ones were missing. In these cases, we could not apply the inverse method to calculate the velocity at the reference level. However, we could still calculate the geostrophic velocity assuming a no-motion reference level. This calculation was carried out considering the see bottom as the no motion reference level. In this case, 42 campaigns were available. The year and month for each of these campaigns are shown in columns 3 to 6 in Table 1.

2.3. Geostrophic velocities and transports in the southern sections. Statistical significance

The total number of oceanographic campaigns in which the closed boxes in the Mallorca and Ibiza Channels were completed was 23 (see section 2.2). However, the number of campaigns when the southern sections of the boxes, crossing both the Mallorca and Ibiza Channels, were completed was much larger: 42. In these cases, transports through the southern sections of the channels were calculated assuming a zero velocity at the reference level which was considered as the sea bottom. In this way, a time series of 42 data points was available. Obviously, the campaigns when the complete boxes were completed, were a sub-set of the larger data set when only the southern sections were available. This

Table 1
Columns 1 and 2 show the year and month for those campaigns when the northern and southern sections of both Mallorca and Ibiza Channels could be completed after interpolation. These are the final campaigns that were used for the calculation of water mass transports by means of circulation inverse models. Columns 3 to 6 show the years and months of the campaigns when only the southern sections of Mallorca and Ibiza Channels could be completed. The water mass transports corresponding to these campaigns were calculated using the geostrophic approximation and considering the sea bottom as the no-motion reference layer.

Campaigns with complete boxes		Campaigns with complete southern sections			
Year	Month	year	Month	year	month
1996	4	1996	4	2009	5
1996	8	1996	6	2011	5
1997	8	1996	8	2013	3
1999	5	1997	8	2013	6
2001	3	1999	5	2013	11
2001	11	2001	3	2014	2
2002	5	2001	11	2014	6
2002	9	2002	3	2015	2
2003	6	2002	5	2015	5
2004	3	2002	9	2016	2
2004	5	2003	6	2016	4
2005	9	2003	10	2016	7
2006	4	2004	3	2016	11
2013	3	2004	5	2017	6
2013	6	2004	10	2017	11
2014	2	2005	3	2018	2
2014	6	2005	9	2019	1
2015	5	2006	4	2022	4
2017	6	2006	6	2022	11
2017	11	2007	10		
2018	2	2008	2		
2019	1	2008	5		
2022	11	2008	7		

allows a comparison of transports calculated from geostrophic velocities estimated using a zero velocity at the bottom of the sea, and transports calculated considering the velocity at the reference level estimated from the inverse method.

Average transports (both from the inverse method and using a zero reference velocity at the sea bottom) were averaged in order to obtain net transports throughout each season of the year. Confidence intervals were estimated for each mean value assuming a T-Student distribution for the mean and using the equation:

$$\frac{s}{\sqrt{n}}T(1-\frac{\alpha}{2},n-1)$$

where s is the sample standard deviation, n is the number of observations, and $n-1$ is the number of degrees of freedom. $T(1-\alpha/2,n\text{-}1)$ is the critical value from the two-tailed inverse cumulative distribution function of the Student's t-distribution, corresponding to a confidence level of $1-\alpha$ and $n\text{-}1$ degrees of freedom. In this work the 95 % confidence level was used (equivalently, the 5 % significance level). Mean or net transports were considered as statistically significant if they were

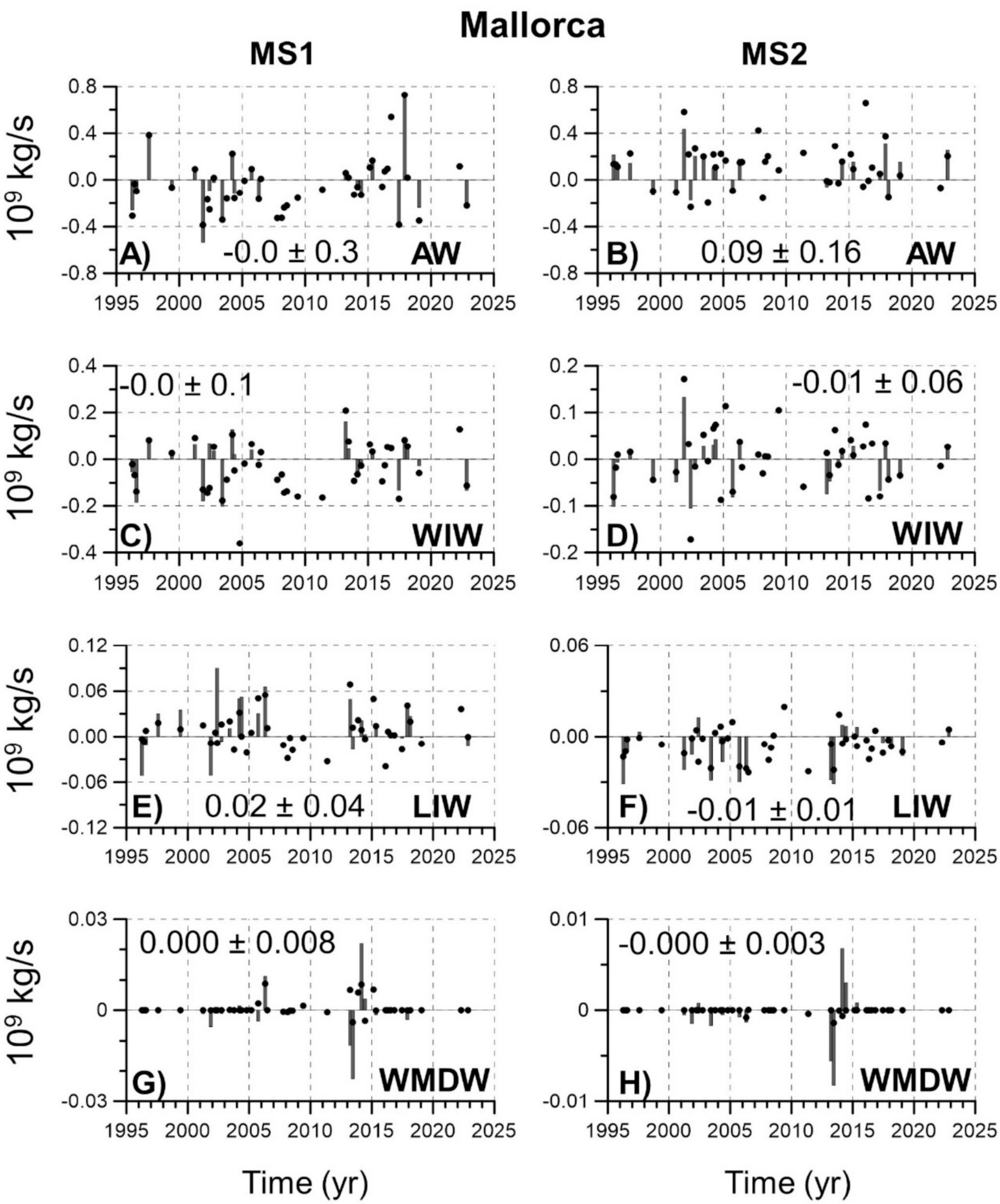

Fig. 2. The left column (Figures A, C, E, G) show the mass transports for the AW, WIW, LIW and WMDW water masses through the MS1 subsection (western subsection of the southern Mallorca Channel). Positive and negative values correspond to northward and southward transports respectively. The right column (Figures B, D, F, H) show the mass transports for the MS2 subsection (the eastern subsection of the southern Mallorca Channel). Grey bars correspond to the results obtained from the application of the inverse model to the closed box of oceanographic stations. Black dots correspond to results from geostrophic velocities obtained using just the southern sections of the channels and the sea bottom as no-motion reference level. Mean values ± standard deviations calculated over the complete period of time are included in the inserts.

different from zero at the 5 % significance level.

3. Results

3.1. Time series of transports through the Balearic Channels

Fig. 2A to H display the mass transports of the four water masses analysed (AW, WIW, LIW, and WMDW) for the MS1 and MS2 subsections of the southern section of the Mallorca Channel, while Fig. 3A to H present analogous results for the IS1 and IS2 subsections of the southern Ibiza Channel. Negative values indicate southward transports whereas positive values indicate a northward transport.

As detailed in Section 2.2, geostrophic velocities and corresponding transports were estimated using inverse modelling to determine the velocity at the reference level. The grey bars represent mass transports derived from this methodology for the 23 campaigns in which both triangular boxes (located in the Ibiza and Mallorca Channels) were fully sampled.

In addition to these, we considered a broader set of campaigns in which all stations along the southern sections of both triangles were

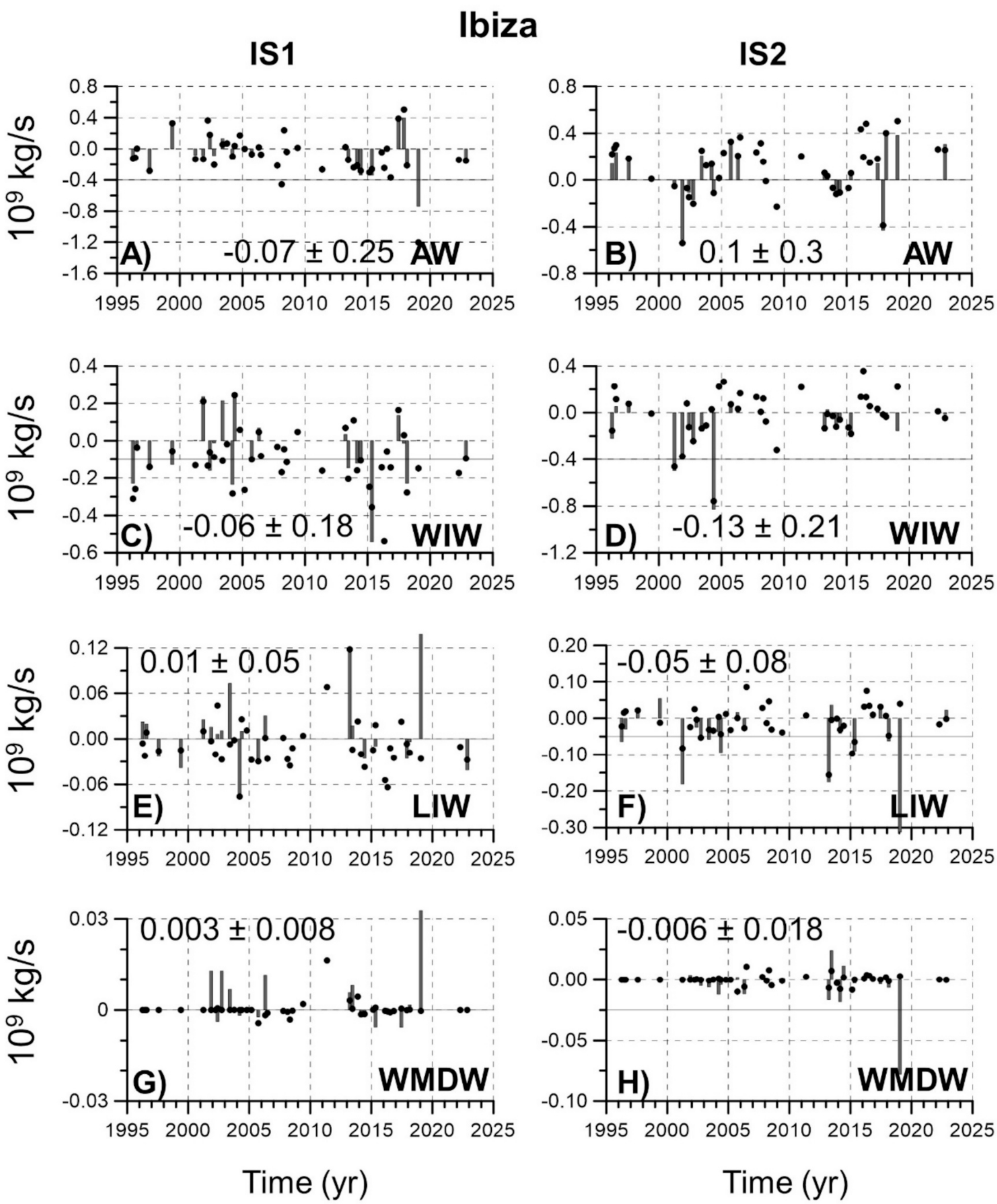

Fig. 3. The left column (Figures A, C, E, G) show the mass transports for the AW, WIW, LIW and WMDW water masses through the IS1 subsection (western subsection of the southern Ibiza Channel). Positive and negative values correspond to northward and southward transports respectively. The right column (Figures B, D, F, H) show the mass transports for the IS2 subsection (the eastern subsection of the southern Ibiza Channel). Grey bars correspond to the results obtained from the application of the inverse model to the closed box of oceanographic stations. Black dots correspond to results from geostrophic velocities obtained using just the southern sections of the channels and the sea bottom as no-motion reference level. Mean values ± standard deviations calculated over the complete period of time are included in the inserts.

completed—specifically, the straight-line segments traversing the Mallorca and Ibiza Channels. This less restrictive criterion yielded a total of 42 campaigns. These campaigns included the previous 23 in which the closed boxes had been completed, as well as additional campaigns in which the boxes had not been completed and, therefore, inverse models could not be applied.

Consequently, for this extended set of 42 campaigns, geostrophic velocities and transports across the southern sections of the Mallorca and Ibiza Channels were calculated under the assumption of zero velocity at the reference level (Section 2.3). The results derived from this approach are represented by black dots in Figs. 2 and 3.

These figures show that the circulation through the Balearic Channels associated with the upper layer formed by AW and WIW is very energetic, with transports for each subsection that can reach values close 0.8 Sv (1 Sv = 10^6 m^3/s) for some particular campaigns. 10^9 kg/s corresponds very closely to a volume transport of 1 Sv, hence, we will use indistinctly 10^9 kg/s or Sv for expressing the transports through the Channels (notice that in one case we refer to mass transport and in the other case to the equivalent volume transport). If the complete southern sections were considered, these values could go up to 1 Sv in some cases. However, the transports have a large variability, as indicated by the standard deviation included in Figs. 2 and 3, and positive and negative values alternate without a clear direction, resulting in much lower mean values (also inserted in Figs. 2 and 3).

The transports for the LIW, both for each campaign, and for the mean value, are an order of magnitude lower than those for the AW and WIW, and the transports for the WMDW are almost zero except for a very few campaigns. Notice that in all the cases the standard deviation is much larger than the mean value (inserts in Figs. 2 and 3).

In the cases of the AW and WIW transports, the values obtained from the application of the inverse method are very close to those calculated using the sea bottom as no-motion reference layer. Notice that the dots and bars show very similar values in Figs. 2 and 3 A, B, C and D. On the other hand, the coincidence for the results from these two different approximations is not so good for the LIW and WMDW (Figs. 2 and 3 E, F, G and H).

Fig. 4 shows the scatter plot of the AW and WIW transports calculated using the inverse method (x-axis) versus those obtained considering the sea bottom as no-motion reference layer (y-axis) and without the use of the inverse modelling. Black filled circles show the results for the sub-sections 1 (MS1 in Fig. 4A and IS1 in Fig. 4B), and open circles correspond to sub-sections 2 (MS2 in Fig. 4A and IS2 in Fig. 4B). In all the cases the regression was significant at the 95 % confidence level with p values lower than 0.01. The variance explained by the linear regression is very high for the AW and WIW (see inserts in Fig. 4).

The correlation was much lower for the LIW (Figure not shown). The regression was statistically significant for three of the subsections (MS1, MS2, IS1, $p = 0.03$), and the variance explained ranged between 0.22 and 0.32 (22 % and 32 %). The regression was not significant for the WMDW for none of the subsections. As already said, transport values were very low and erratic for this deep water mass.

3.2. Seasonal mean transports through the Balearic Channels

Although mean transports have been presented for the complete time series in Figs. 2 and 3, these values could be affected by a seasonal cycle.

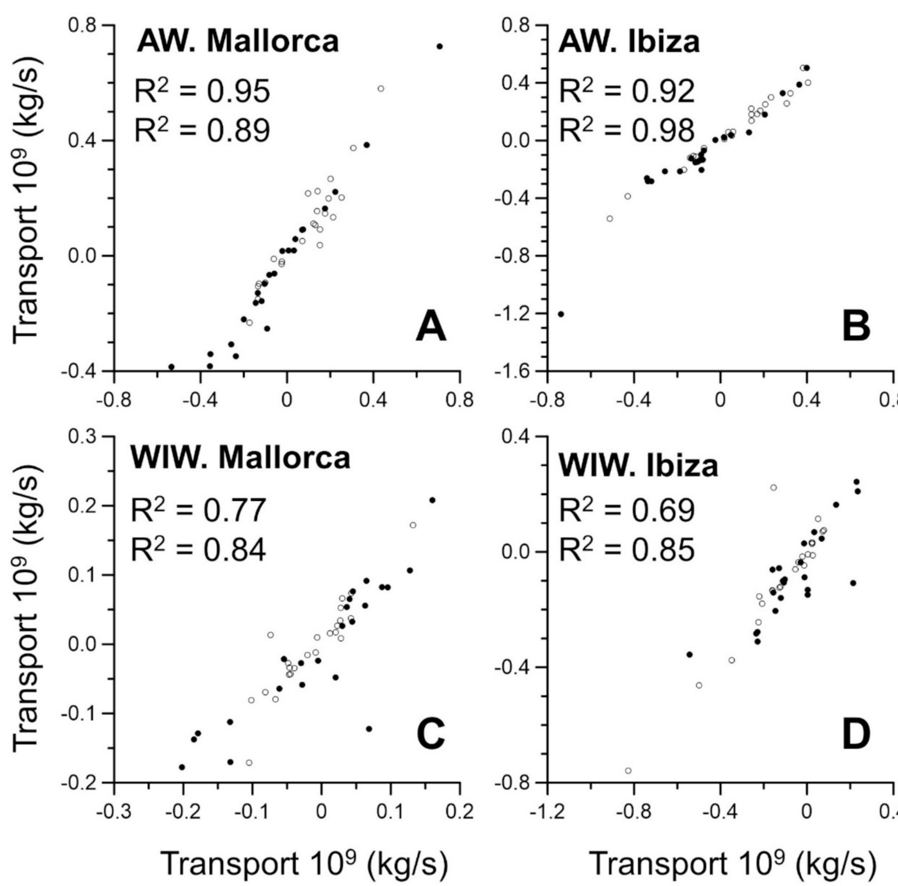

Fig. 4. Fig. 4A shows the regression of AW mass transports calculated by means of the inverse model on mass transports calculated from geostrophic velocities using the sea bottom as no-motion reference level. Black filled circles correspond to the transports through the MS1 subsection and open circles to the MS2 subsection. The inserts show the variance explained by the linear regression for both subsections (upper insert for MS1 and lower insert for MS2). Fig. 4B is the same for the Ibiza Channel (subsections IS1 and IS2) and Fig. 4C and D are the same for the WIW and the Mallorca and Ibiza Channels respectively.

For this reason, mean transports were broken down by season of the year, water mass, and for the four subsections that form the closed triangles in both the Mallorca and Ibiza Channels. Winter was considered as January, February and March, spring as April, May and June, summer as July, August and September, and autumn as October, November and December. Figs. 5, 6, 7 and 8 show these transports for the AW, WIW, LIW and WMDW respectively. Solid lines indicate those mean values that were significant at the 95 % confidence level, whereas dashed lines are used for those mean values that were not statistically significant (not different from zero at the 95 % confidence level). Table 2a–2d shows the mean values and confidence intervals for each season of the year and for all the water masses and subsections.

The winter AW transports show values larger than 0.2 Sv along the peninsular continental slope (see Fig. 5). A large fraction of this flow seems to cross the Ibiza Channel through its western sector, whereas there is a northward intrusion of AW through the eastern Ibiza Channel, reinforcing the Balearic Current that flows along the northern slope of the Mallorca Channel. The water mass exchange at the southern section of Mallorca Channel suggests an anticyclonic character of the circulation. The mean winter transports for the WIW also show a value larger than 0.2 Sv close to the peninsular slope which crosses southwards through the southern section of the Ibiza Channel. This water mass also contributes to the winter Balearic Current to the north of the Mallorca Channel. The LIW flows southwards through the Ibiza Channel with a transport of 0.11 Sv (= 0.14 Sv–0.03 Sv, see inserts in Fig. 7). North and southward transports through both Channels suggest eddy activity. The presence of these structures within the channels would produce recirculation of this water mass and the change of direction of the transport within the channels without a clear sign of the net contribution of LIW to the Balearic Current. The winter transport of WMDW shows a net southward transport of −0.01 Sv. However, this value is not statistically significant and is zero for the rest of the seasons. Therefore, the transports of this water mass will not be commented on following paragraphs.

In spring, the AW does not show the existence of the Balearic Current and the net southward transport is very low (0.02 Sv), being the Mallorca Channel the main path of this transport. Southward and northward WIW transports at the northern side of the Ibiza Channel suggest a strong anticyclonic circulation. The southward transport through the southern section in this channel would indicate the detachment of 0.22 Sv from this anticyclonic circulation (Fig. 6). This transport would be similar to that observed during winter. The circulation of this water mass seems to be dominated by mesoscale eddy activity with no evidence of the presence of the Balearic Current. However, a southward transport of −0.04 Sv is observed in the southern section of Mallorca Channel, but this value is not statistically significant. LIW does not follow a clear pattern. The northward transports in the western sides of both channels, and the southward ones on the eastern sides, on both the northern and southern sections, could indicate the prevalence of an anticyclonic circulation.

The AW summer circulation shows the presence of the Balearic Current at the northern section of the Mallorca Channel (0.31 Sv), as in winter. However, during this season, this current cannot be tracked westwards to the peninsular continental slope, as during winter, and it has important contributions of AW flowing northwards through the Mallorca Channel. The WIW also follows the Balearic Current at the northern Mallorca Channel, but with a lower transport (~0.1 Sv). A southward transport of WIW close to −0.1 Sv is observed in the Ibiza Channel. However, it should be noticed that none of these values were statistically significant. Finally, summer LIW transports were dominated by an anticyclonic circulation in both Channels, with a small (−0.02 Sv) and not significant southward contribution through the Ibiza Channel.

The autumn AW circulation is quite similar to that observed in winter. A −0.2 Sv transport is observed at the peninsular side of the Ibiza Channel, and most of this water mass flows southwards through the Channel. The Balearic Current transport at the northern slope of Mallorca Channel is 0.49 Sv with a large contribution of AW flowing northwards through the Mallorca Channel. WIW also flows to the south through the Ibiza Channel with a net transport of −0.09 Sv and an anticyclonic circulation in the southern section of 0.04 Sv. WIW also contributes to the Balearic Current with a transport of 0.08 Sv at the northern section of Mallorca Channel and some eddy activity in the southern section. The LIW shows no evidence of contributing to the Balearic Current and has a southward transport of −0.01 Sv in both the Ibiza and Mallorca Channels (although not significant).

3.3. Circulation modes

In addition to the large standard deviations of transports (see Figs. 2

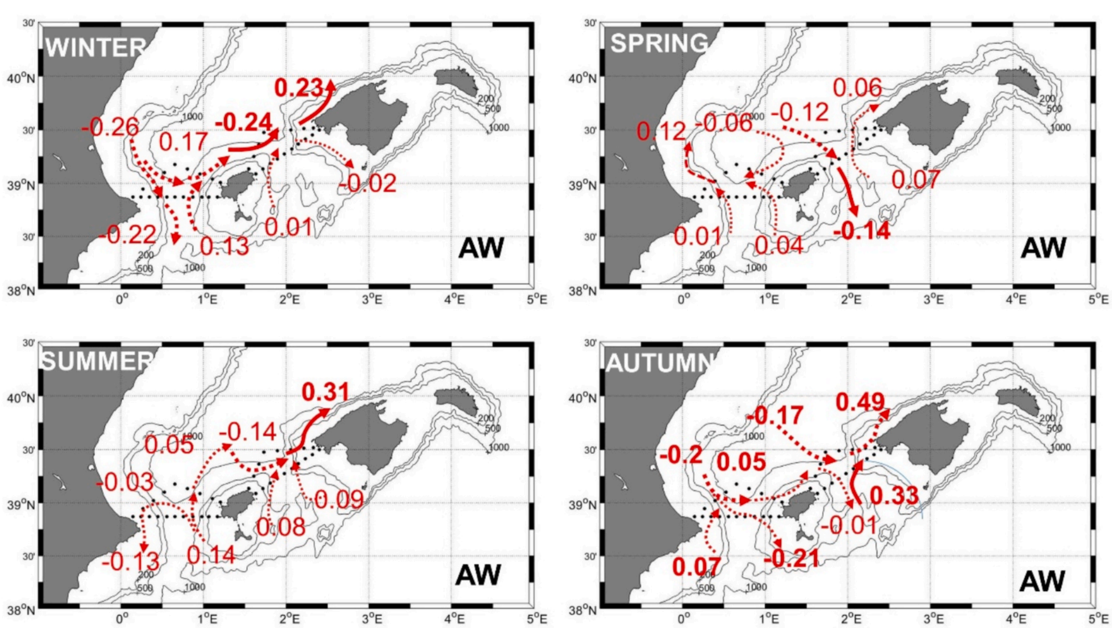

Fig. 5. Mean mass transports expressed in 10^9 kg/s (~1 Sv) for winter, spring, summer and autumn. Solid lines and bold numbers are used for those mean values that are statistically significant at the 95 % confidence interval and dashed lines correspond to non-significant results.

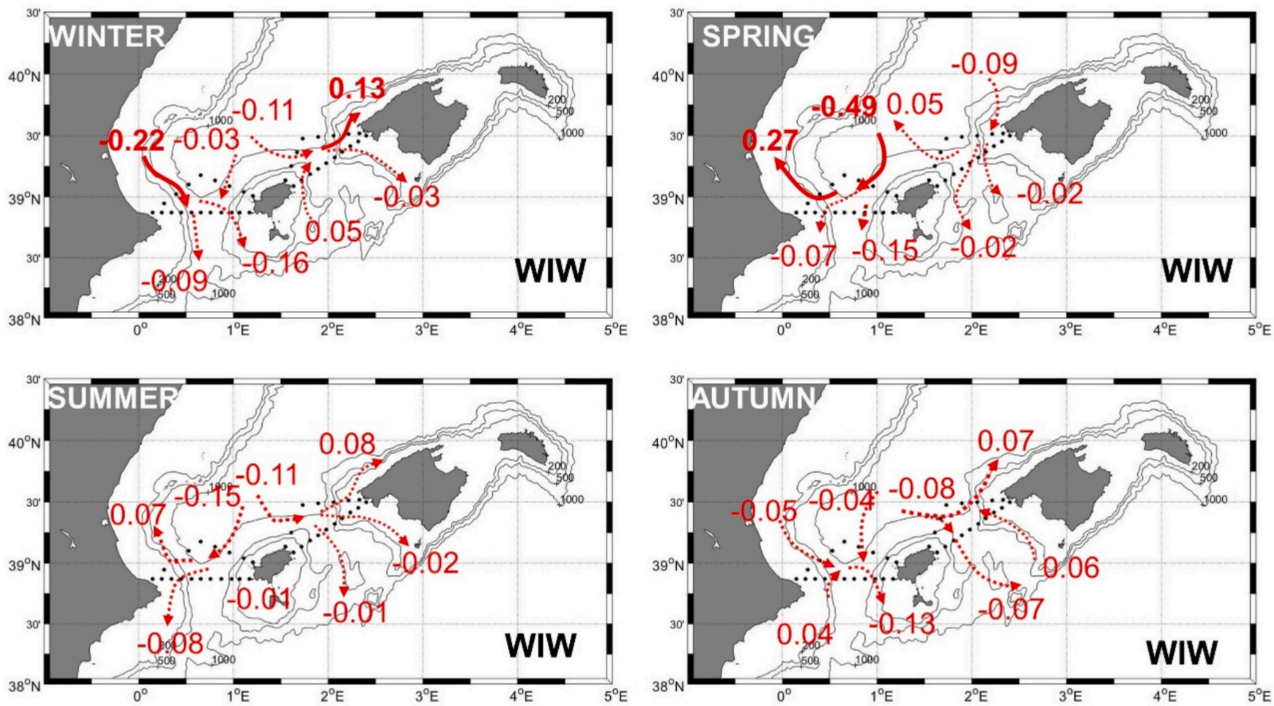

Fig. 6. The same as in Fig. 5, but for the WIW.

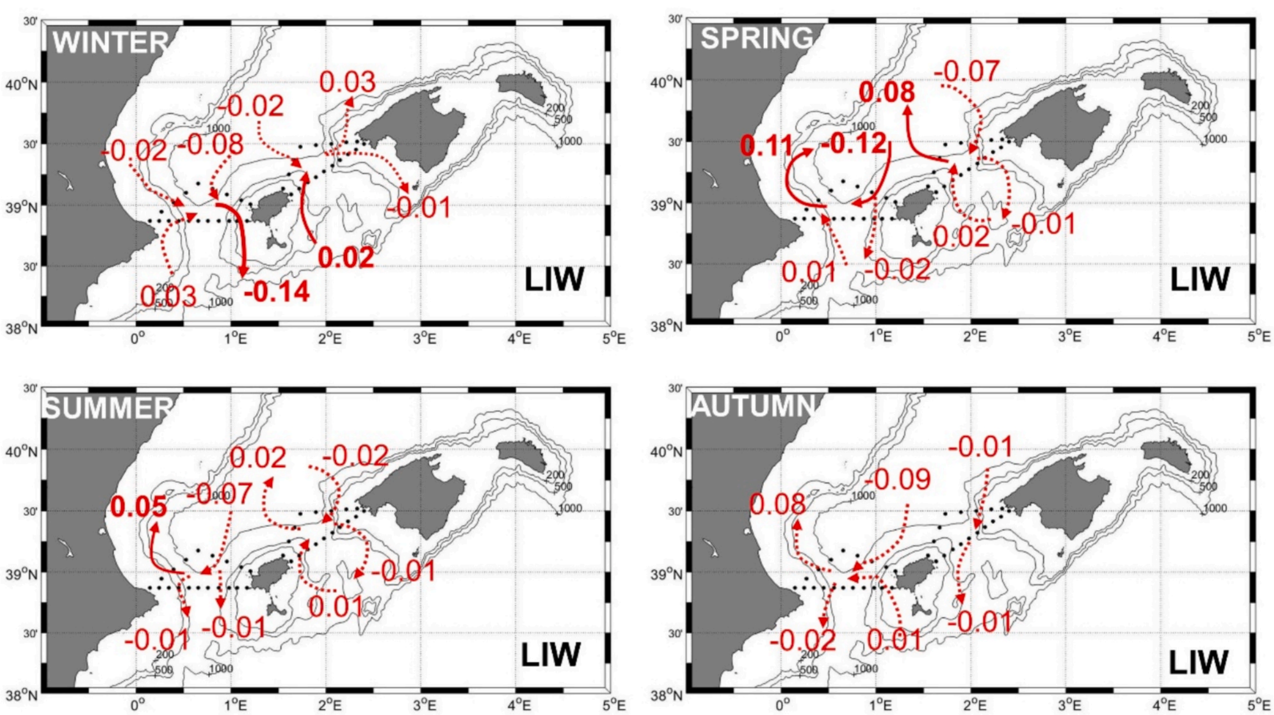

Fig. 7. The same as in Fig. 5, but for the LIW.

and 3), the variability of the circulation in the Balearic Channels is reflected by the existence of different "modes" of circulation. Barceló-Llull et al. (2019) and Heslop et al. (2012) considered three modes of circulation which could be named as, two-way circulation, Northern Current mode and inflow mode. In this work we have identified two more circulation modes that could be named as reversed two-way circulation mode and multiple-eddies mode. Fig. 9 shows four situations in which the first four circulation modes have been clearly identified for the upper layer of the Ibiza Channel (surface to 300 m: AW and WIW). It should be noticed that the same modes of circulation have been established for the Mallorca Channel. Fig. 9A and B show an example of the two-way circulation mode in the Ibiza Channel corresponding to January 2019. We have considered that the circulation in any of the two Balearic Channels followed this pattern when a clear zero velocity area was located in the central part of the channel and southward velocities (blue dashed lines) were observed in the western part of the channel and northward

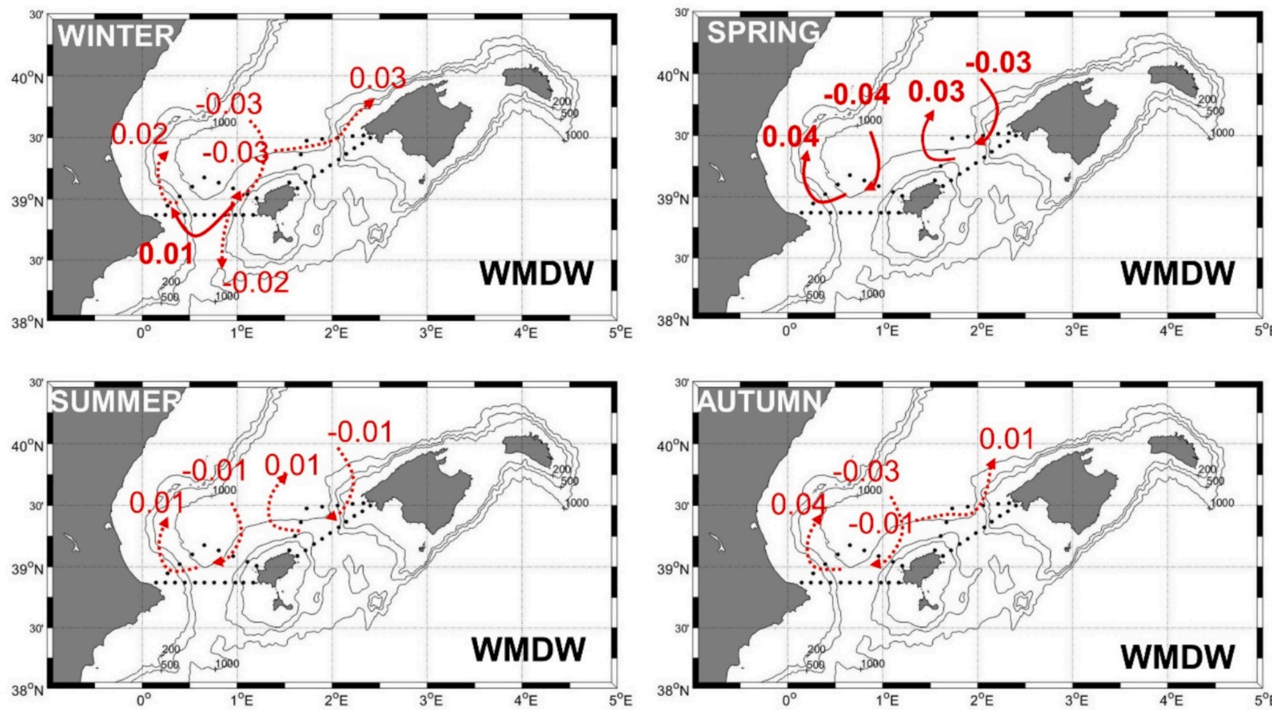

Fig. 8. The same as in Fig. 5, but for the WMDW.

Table 2a
Seasonal mean mass transports in 10^9 kg/s (~1 Sv) and confidence intervals at the 95 % confidence level for the AW. The upper lines correspond to the southern (MS1, MS2) and northern (MN1, MN2) Mallorca sections. The lower lines correspond to the southern (IS1, IS2) and northern (IN1, IN2) Ibiza sections.

AW(mean)	MS1	IC	MS2	IC	MN1	IC	MN2	IC
winter	0.01	0.16	−0.02	0.13	−0.24	0.17	0.23	0.20
spring	−0.14	0.12	0.07	0.10	−0.12	0.15	0.06	0.16
summer	0.08	0.33	0.09	0.21	−0.14	0.20	0.31	0.29
autumn	−0.01	1.59	0.33	0.23	−0.17	0.49	0.49	1.53
	IS1	**IC**	**IS2**	**IC**	**IN1**	**IC**	**IN2**	**IC**
winter	−0.22	0.28	0.13	0.24	−0.26	0.31	0.17	0.19
spring	0.01	0.17	0.04	0.09	0.12	0.18	−0.06	0.07
summer	−0.13	0.21	0.14	0.34	−0.03	0.32	0.05	0.44
autumn	0.07	0.72	−0.21	1.12	−0.20	1.05	0.05	0.63

Table 2b
Seasonal mean mass transports in 10^9 kg/s (~1Sv) and confidence intervals at the 95 % confidence level for the WIW. The upper lines correspond to the southern (MS1, MS2) and northern (MN1, MN2) Mallorca sections. The lower lines correspond to the southern (IS1, IS2) and northern (IN1, IN2) Ibiza sections.

WIW(mean)	MS1	IC	MS2	IC	MN1	IC	MN2	IC
winter	0.05	0.09	−0.03	0.04	−0.11	0.09	0.13	0.12
spring	−0.02	0.06	−0.02	0.04	0.05	0.16	−0.09	0.17
summer	−0.01	0.19	−0.02	0.06	−0.11	0.13	0.08	0.17
autumn	−0.07	0.36	0.06	0.15	−0.08	0.47	0.07	0.40
	IS1	**IC**	**IS2**	**IC**	**IN1**	**IC**	**IN2**	**IC**
winter	−0.09	0.13	−0.16	0.19	−0.22	0.16	−0.03	0.15
spring	−0.07	0.17	−0.15	0.18	0.27	0.31	−0.49	0.16
summer	−0.08	0.11	−0.01	0.23	0.07	0.24	−0.15	0.37
autumn	0.04	0.43	−0.13	0.47	−0.05	0.34	−0.04	0.23

velocities (red solid lines) were observed in the eastern part of it. This velocity field is associated to a density dome-shaped structure in the central part of the channel (Fig. 9A). In addition to this, we have observed a second two-way mode (Fig. 9C and D) in which the northward velocity is observed on the western side of the channel and the southward velocities occurred along its eastern side (Fig. 9D). This circulation pattern is associated with the sinking of isopycnals in the central part of the channel (Fig. 9C) and could be named as reversed two-way circulation mode. Notice that a zero velocity area and a reversal of the currents were usually observed in the coastal zones of the channels (see Fig. 9B, D, F, H). However, the two-way circulation mode has been considered in this work only when the change of direction of

Table 2c
Seasonal mean mass transports in 10^9 kg/s (~1Sv) and confidence intervals at the 95 % confidence level for the LIW. The upper lines correspond to the southern (MS1, MS2) and northern (MN1, MN2) Mallorca sections. The lower lines correspond to the southern (IS1, IS2) and northern (IN1, IN2) Ibiza sections.

LIW(mean)	MS1	IC	MS2	IC	MN1	IC	MN2	IC
winter	0.02	0.02	−0.01	0.01	−0.02	0.04	0.03	0.04
spring	0.02	0.03	−0.01	0.01	0.08	0.05	−0.07	0.08
summer	0.01	0.04	−0.01	0.02	0.02	0.09	−0.02	0.11
autumn	−0.01	0.11	0.00	0.02	0.00	0.10	−0.01	0.22
	IS1	**IC**	**IS2**	**IC**	**IN1**	**IC**	**IN2**	**IC**
winter	0.03	0.08	−0.14	0.11	−0.02	0.17	−0.08	0.13
spring	0.01	0.02	−0.02	0.04	0.11	0.09	−0.12	0.07
summer	−0.01	0.04	−0.01	0.06	0.05	0.05	−0.07	0.08
autumn	−0.02	0.07	0.01	0.03	0.08	0.13	−0.09	0.17

Table 2d
Seasonal mean mass transports in 10^9 kg/s (~1Sv) and confidence intervals at the 95 % confidence level for the WMDW. The upper lines correspond to the southern (MS1, MS2) and northern (MN1, MN2) Mallorca sections. The lower lines correspond to the southern (IS1, IS2) and northern (IN1, IN2) Ibiza sections.

WMDW(mean)	MS1	IC	MS2	IC	MN1	IC	MN2	IC
winter	0.00	0.01	0.00	0.00	−0.03	0.05	0.03	0.05
spring	0.00	0.01	0.00	0.00	0.03	0.02	−0.03	0.02
summer	0.00	0.00	0.00	0.00	0.01	0.02	−0.01	0.03
autumn	0.00	0.01	0.00	0.00	−0.01	0.05	0.01	0.04
	IS1	**IC**	**IS2**	**IC**	**IN1**	**IC**	**IN2**	**IC**
winter	0.01	0.01	−0.02	0.03	0.02	0.14	−0.03	0.13
spring	0.00	0.00	0.00	0.01	0.04	0.04	−0.04	0.04
summer	0.00	0.01	0.00	0.00	0.01	0.03	−0.01	0.03
autumn	0.00	0.02	0.00	0.01	0.04	0.10	−0.03	0.12

the current was observed in the central part of it. Fig. 9E and F show a clear situation of the northern current mode. In this case the central part of the channel is occupied by a southward current. Once again we emphasize that this classification is made according to the circulation in the central part of the channel, but usually a recirculation occurs on the shelves of both sides of it. This circulation mode is associated to a downward tilt to the west of the isopycnals (Fig. 9E). Finally, Fig. 9G and H illustrate the inflow circulation mode. In this case, the central part of the channel is occupied by a northward current and the isopycnals sink to the east. The fifth circulation mode (multiple-eddies mode) was exceptionally observed (not shown) and was characterized by an intense mesoscale activity with continuous reversals in the direction of the flow along the whole width of the channel.

It should be noted that we have restricted this analysis to the upper 300 m of the water column where AW and WIW flow. There are two reasons for limiting this description to this upper layer. First, this is the most energetic layer as evidenced by the large transports presented in Figs. 2 and 3. Second, the geostrophic velocities corresponding to this upper layer, obtained using the sea bottom as no-motion reference layer, are in good agreement with those obtained by means of the circulation inverse methods (Fig. 4). Therefore, the use of the former velocities allows us to increase the number of campaigns for their statistical analysis (42 campaigns instead of 23; see sections 2.2 and 2.3). Fig. 10 summarizes the results of this analysis. Fig. 10A to 10D show in a schematic way the relative frequency (expressed as percentages) corresponding to the observations of the first four circulation modes described in Fig. 9 for the Ibiza and Mallorca Channels. Fig. 10A and 10B show the relative frequency of observations for the two-way and reversed two-way circulation modes. Fig. 10C corresponds to the relative frequency of the Northern Current circulation mode, and Fig. 10D is for the inflow mode. The 5 % and the 7 % of the campaigns could not be classified in the Ibiza and Mallorca Channels respectively. Besides this, 10 % of the campaigns in the Ibiza Channel and 5 % of them in the Mallorca Channel, showed the multiple-eddies mode of circulation. The only reason for not representing this latter mode in Fig. 10 is the difficulty to make a schematic representation of this circulation pattern. It is also important to clarify that the schematic representation of Fig. 10 does not mean that the different circulation modes occur simultaneously on both channels. For instance, Fig. 10A shows that there is a two-way circulation mode in the Ibiza Channel 40 % of the campaigns and this circulation mode is observed 38 % of the occasions in the Mallorca Channel. However, these circulation modes do not necessarily occur simultaneously. The five circulation modes described above are observed in many different combinations in both channels.

However, Fig. 10 shows that the most frequent situation in both channels is a two-way circulation with the upper layer flowing southwards in the western side of the channel and northward on the eastern side of it. The inflow and the northern current would be the following most frequent modes. Nevertheless, the application of a Chi-squared test (see Zar, 1984 for instance) revealed no statistically significant differences for the frequencies at which these two modes were observed. The frequency associated with each circulation mode was also calculated for each season of the year. The two-way circulation mode was also the most frequent one during the four seasons of the year and for both channels, but no significant differences could be found as the number of campaigns for each season of the year is still very low: 11 for winter, 17 for spring, 6 for summer and 8 for autumn (see Table 1).

4. Discussion

In this work we have calculated the water transports through the Ibiza and Mallorca Channels by means of an inverse method using temperature and salinity data from 23 oceanographic campaigns extending from 1996 to 2022. Then, mean seasonal transports have been calculated averaging those values corresponding to each season of the year. This procedure is different from that used in Vargas-Yáñez et al. (2020) where the transports associated to the mean seasonal temperature and salinity fields were calculated. Despite the extension of the time series from 2019 to 2022, a comparison between both methods could be accomplished.

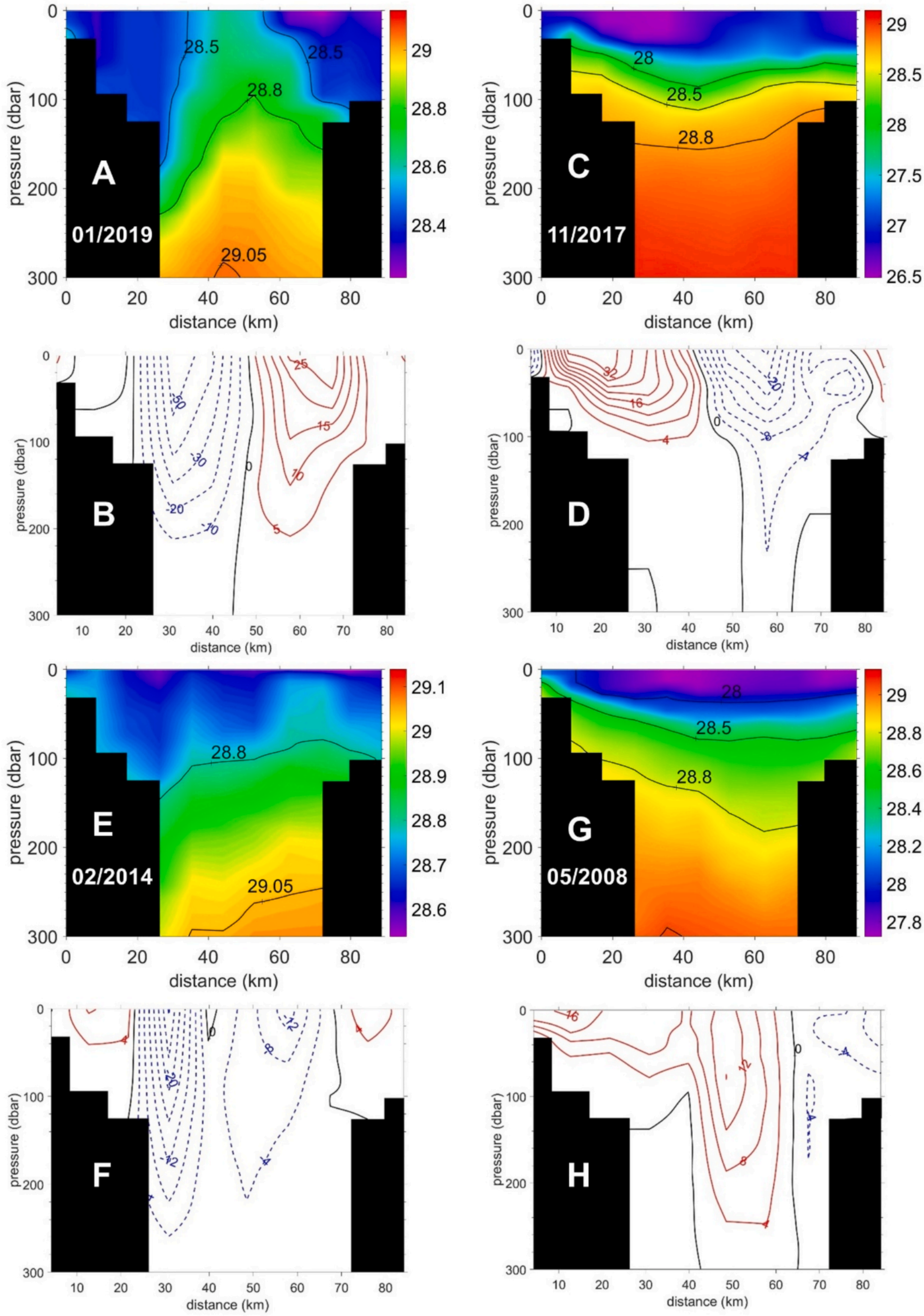

Fig. 9. Fig. 9A and B show the density and geostrophic velocity fields at the Ibiza Channel corresponding to the January 2019 survey. Blue dotted lines in Fig. 9B, D, F, H indicate negative southward velocities whereas red solid lines indicate positive northward velocities expressed in cm/s. This situation has been considered as representative of the two-way circulation mode described in this work. In this case southward velocities occur at the western side of the channel and northward velocities are observed in the eastern side. Fig. 9C and D correspond to the November 2011 cruise and is considered as an example of the reversed two-way circulation mode in which currents flow in opposite direction to those of the two-way circulation. Fig. 9E and F from the February 2014 survey are an example of the Northern Current circulation mode, and Fig. 9G and H illustrate the inflow circulation mode during May 2008. Notice that recirculation is usually observed in the coastal sides of the channels. Geostrophic velocities in this figures have been calculated assuming a zero reference velocity at the sea bottom. (For interpretation of the references to colour in this figure legend, the reader is referred to the web version of this article.)

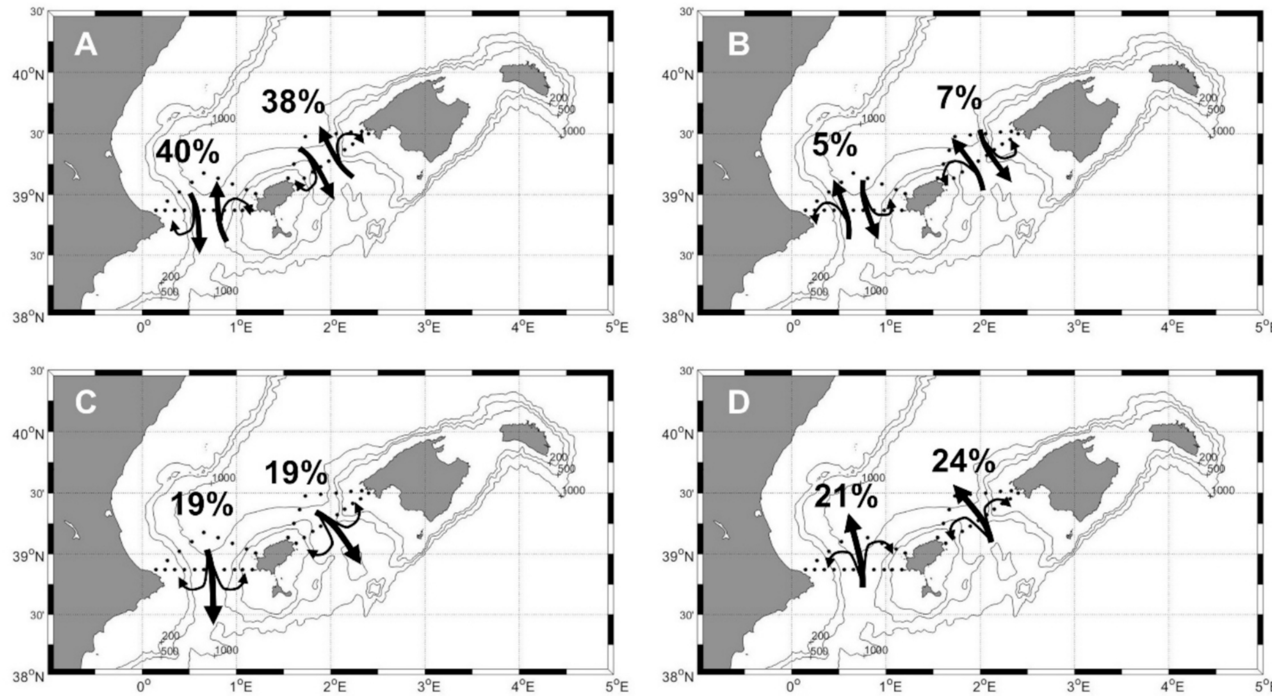

Fig. 10. Schematic representation of the percentages associated with four of the modes of circulation in the Ibiza and Mallorca Channels. Fig. 10A corresponds to the two-way circulation mode with southward transport at the western side and northward transport at the eastern side of the channel. Fig. 10B corresponds to the reversed two-way circulation mode with northward transport at the western side and southward transport at the eastern side of the channel. Fig. 10C corresponds to the Northern Current mode and Fig. 10D to the inflow mode. The multiple-eddy mode has not been represented. Thin black lines have been included in all the cases to indicate the frequent recirculation in the coastal areas.

Tables 3a and 3b shows the transports for the upper layer (AW + WIW) for the two western (MS1, IS1) and eastern (MS2, IS2) subsections of the southern Mallorca and Ibiza Channels. The total net transports for each channel are also presented (fourth column in Tables 3a and 3b). The values calculated in Vargas-Yáñez et al. (2020) have been included in parenthesis for comparison in both Tables 3a and 3b. Table 3a corresponds to the results obtained using the inverse method and Table 3b shows the results using the geostrophic velocities with the no-motion reference layer at the sea bottom.

There is a qualitative agreement between the transports calculated for the complete sections (column 4 in Tables 3a and 3b), but not for each subsection (eastern and western parts of the channels, columns 2 and 3 in Tables 3a and 3b). Whether the inverse method is used (Table 3a) or not (Table 3b), the results show a northward net transport of the upper layer in the Mallorca Channel throughout the year, with the only exception of spring, when the net transport is directed to the south. In the Ibiza Channel, the net transports are directed to the south during all the seasons of the year. The only exception would be the summer value when the time series of transports are calculated using the geostrophic velocities without the use of the inverse method (Table 3b). If the four seasons of the year are averaged, the results for the complete sections show a mean annual northward transport ranging between 0.07 and 0.09 Sv for the Mallorca Channel, whereas the annual mean transport for the Ibiza one would range between −0.1 and −0.21 Sv (southwards).

Table 3a
Mean transports in 10^9 kg/s (~1 Sv) for the upper layer made of the AW and WIW from the 23 complete campaigns in which the inverse model could be applied. The transports are calculated for the western (MS1, IS1) and eastern sectors (MS2, IS2) of the southern sections of Mallorca and Ibiza Channels (columns 2 and 3) and for the complete section (column 4). Mean transports from Tables 3a and 3b in Vargas-Yáñez et al. (2020) are included in parenthesis for comparison.

AW + WIW	MS1	MS2	MS
winter	0.06(0.01)	−0.05(0.09)	0.01(0.10)
spring	−0.16(−0.14)	0.05(0.09)	−0.11(−0.05)
summer	0.07(−0.01)	0.07(0.13)	0.14(0.13)
autumn	−0.08(−0.06)	0.39(0.17)	0.31(0.12)
	IS1	**IS2**	**IS**
winter	−0.31(−0.41)	−0.03(0.1)	−0.34(−0.33)
spring	−0.06(−0.27)	−0.11(0.1)	−0.17(−0.18)
summer	−0.21(−0.29)	0.13(0.15)	−0.08(−0.14)
autumn	0.11(−0.14)	−0.34(0.1)	−0.23(−0.03)

Table 3b
The same as in Table 3a, but using the transports calculated from geostrophic velocities assuming a no-motion reference layer at the sea floor.

AW + WIW	MS1	MS2	MS
winter	−0.03(0.01)	0.04(0.09)	0.01(0.10)
spring	−0.16(−0.14)	0.10(0.09)	−0.06(−0.05)
summer	0.05(−0.01)	0.10(0.13)	0.15(0.13)
autumn	−0.09(−0.06)	0.28(0.17)	0.19(0.12)
	IS1	**IS2**	**IS**
winter	−0.37(−0.41)	0.15(0.1)	−0.22(−0.33)
spring	−0.14(−0.27)	0.07(0.1)	−0.07(−0.18)
summer	−0.19(−0.29)	0.21(0.15)	0.02(−0.14)
autumn	−0.04(−0.14)	−0.05(0.1)	−0.09(−0.03)

Barceló-Llull et al. (2019) pointed out that the inter-annual and high frequency variability of the circulation in the Balearic Channels was much larger than the seasonal signal. The results presented in this work (Figs. 2 and 3) and the large standard deviations for the AW and WIW which range between 0.2 and 0.3 Sv support this previous result. This large variability obscures the calculation of the seasonal mean values as well as the annual mean values which are not statistically significant in many of the cases (Table 2a–2d). However, the coincidence, at least from a qualitative point of view, between different methodologies, supports one of the results presented in this and previous works. That is, in the upper layer, a northward water transport prevails in the Mallorca Channel year-round, with an intensification of this flow during autumn, while a southward transport dominates in the Ibiza Channel, with intensification in winter.

The agreement between the different methodologies is not so good from a quantitative point of view. First, it should be noted that the mean seasonal transports calculated by means of inverse models and using the sea-bottom as no motion reference layer show some differences (although the direction of the flow is coincident; compare Tables 3a And 3b). However, Fig. 4 shows the high correlation between the results obtained using these two methodologies for the AW and WIW transports. In the case of these two water masses, the mean R^2 coefficient (variance explained) was 0.86 and values ranged between 0.65 and 0.98 depending on the season of the year and the section considered. Barceló-Llull et al. (2019) and Heslop et al. (2012), following Pinot et al. (1995), used the 800 m level as no-motion layer and the sea-bottom in shallower waters for the calculation of geostrophic velocities. These authors showed that the use of the 900 m level as reference layer introduced no significant changes in the results. In the present study the sea-bottom was used as no-motion level. It should be noticed that most of the oceanographic stations in the Balearic Channels are shallower than 900 m (see Table S1) and therefore our choice is quite similar to that of previous works. The good agreement with the inverse method results show that the current velocities at deep levels of the Balearic Sea are certainly very low compared to those observed at the upper 300 m and therefore the use of 800, 900 m or the sea bottom as reference layer are adequate choices. Furthermore, the application of the inverse method allowed us to obtain velocities at the sea bottom of the order of 1–2 cm/s (not shown), and Pinot et al. (2002) found velocities between 0 and very few centimetres per second in current measurements close to the sea bottom, supporting our reference level choice. Taking into account this good agreement between the transports calculated in the upper 300 m with and without the use of inverse modelling, we can conclude that the differences in the seasonal and annual mean transports obtained from both methodologies are due to the use of a different number of campaigns: 23 in one case and 42 in the other. These differences are enhanced by the large high frequency and inter-annual variability and the still low number of campaigns.

These results could have important implications for understanding a more general picture of the WMED circulation. Considering the sum of the upper layer transports (AW + WIW) at the Ibiza and Mallorca Channels (Tables 3a and 3b), they contribute to the north–south water exchange in the WMED with a net southward transport ranging between −0.02 and −0.12 Sv (depending on the methodology used). Let us consider the Northwestern Mediterranean limited by the Balearic Channels, a west-east line extending from Menorca Island to Sardinia, the Corsica Strait and the coasts of Italy, France and Spain. If we accept that the water flux between Mallorca and Menorca (shallow waters) and at the Bonifacio Strait (between Sardinia and Corsica) are negligible, then the mass conservation of the upper layer (AW + WIW) requires a balance between the inflow of water through the Corsica Channel, the water exchange through the Mallorca and Ibiza Channels, the water exchange through the Menorca-Sardinia section, the fresh water deficit in this region and the volume of AW contributing to the deep water formation at the Northwestern Mediterranean. The surface water flux through the Corsica Strait is highly variable, being intense in winter and spring and negligible in summer (Astraldi and Gasparini, 1994). Béranger et al. (2005) found an annual mean value of 0.5 Sv using a numerical model, being this value close to the climatological value reported in this same work (0.47 Sv). The formation of deep water is very variable, alternating years with strong deep convection with other years when this process is absent (Margirier et al., 2020; Herrmann et al., 2010). However, it is usually accepted that the mean value is around 0.3 Sv (Poulos, 2023; Lascaratos, 1993). More recent numerical simulations yielded a mean value of 0.35 Sv (Somot et al., 2018). The AW would contribute with a 25 % or 33 % to the formation of the WMDW, being the LIW the contributor for the rest of the deep water volume (Millot and Taupier-Letage, 2005; Bethoux, 1980). We will consider those water transports into the Northwestern Mediterranean as positive and those exiting this area as negative. If Q_{CH} is the water transport for the Mallorca and Ibiza Channels, Q_{MS} is the transport for the Menorca-Sardinia section, Q_{CS} is the transport through the Corsica Strait and the fresh water deficit for this region is 0.007 Sv, this balance could be written as:

$Q_{CS} + Q_{CH} + Q_{MS} - 0.007–0.33x0.35 = 0$ where we have considered the deep water formation rate obtained by Somot et al. (2018) and a 33 % contribution of the upper layer.

Using the value 0.5 Sv for the Q_{CS} (Corsica Strait), then:

$$Q_{CH} + Q_{MS} = -0.38Sv$$

Therefore, the knowledge of the net annual transport through the Balearic Channels could be used to infer the water exchange through the Menorca-Sardinia section. It should be stressed that Ribotti et al. (2004) found that the surface water flows eastwards to the south of the Sardinian Channel (between Sardinia and Tunicia) and to the west at the northern section of this channel. Astraldi and Gasparini (1994) showed that the surface AW recirculates cyclonically in the Tyrrhenian Sea during summer, flowing out of the Tyrrhenian Sea at the southern tip of Sardinia. Bethoux (1980) concluded from mass and salt conservation equations that there was a northward net transport of 0.37 or 0.15 Sv through the Menorca-Sardinia section (depending on the transport considered in the Gibraltar Strait). These calculations assumed a southward transport through the Ibiza Channel between −0.37 and −0.58 Sv. No fluxes were considered in that work for the Mallorca Channel and hence, the Ibiza Channel value is supposed to represent the net transport through the Balearic Channels. These works make us hypothesize that the AW entering the Tyrrhenian Sea, partially flows to the north finally crossing the Corsica Strait and partially recirculates cyclonically within the Tyrrhenan Sea to finally exit through the southern tip of Sardinia. Then, this water mass would turn to the north and the average transport of AW at the region located to the west of Sardinia would be directed to the north. This AW flow would finally join the surface water crossing the Corsica Strait to form the Northern Current. This northward AW current along the western coast of Sardinia would follow the same path as the LIW (Millot and Taupier-Letage, 2005). As opposed to this hypothesis, it should be taken into account that, despite the high transports that could be observed during some specific campaigns, the annual mean values obtained in the present work for the Balearic Channels are between −0.02 and −0.12 Sv. This would imply that there is a southward transport through the Menorca-Sardinia section ranging between −0.26 and −0.36 Sv. This would be in agreement with the existence of the Western Mid Mediterranean Current flowing from the northern slope of the Balearic Islands to the southeast and finally into the Sardinian Channel (Cotroneo et al., 2021). These authors used data from drifters and satellite altimetry and their results were coincident with those from numerical models (Pinardi et al., 2015; Olita et al., 2015). However, in our opinion, they would be in contradiction with the results from Knoll et al. (2017). In this latter work, ADCP data showed the existence of the Western Sardinian Current (WSC) flowing to the south along the western coast of Sardinia, but they also showed the prevalence of a northward current at the open sea to the west of Sardinia. It is also difficult to reconcile the existence of the Western Mid Mediterranean Current flowing to the southeast at the southwestern tip of Sardinia with the existence of the Eastern Algerian Gyre which flows cyclonically with a northwest direction at this location (Mallil et al., 2022; Escudier et al., 2016; Testor et al., 2005). The present work cannot solve these apparent contradictions, but stresses the need for better estimations of mass transports through the main passages of the WMED.

As already mentioned, there is a qualitative agreement for the different methodologies used when the net transports trough the complete sections of the channels are considered, but there is no agreement when the subsections are taken into account. Furthermore, the circulation schemes that could be inferred from the mean seasonal transports through the 8 subsections and depicted in Figs. 5 and 6 do not coincide with the most frequently observed circulation modes (Figs. 9 and 10). For instance, the AW autumn circulation in the Ibiza Channel inferred from the mean transports suggests a northward flow in the western section of the channel and a southward flow at the eastern one, whereas this circulation mode is very infrequent at the Ibiza Channel as it was observed just once in autumn and twice in the complete time series. This fact makes us consider that mean transports and currents do not necessarily reflect the main or more frequent circulation patterns in the Balearic Channels and very likely in other parts of the WMED. For instance, just for the sake of discussion, let us consider that the circulation of the upper layer in the Ibiza Channel had a bimodal character (we have already shown that this is not the case) in which the circulation alternates between a Northern Current mode and an inflow mode.

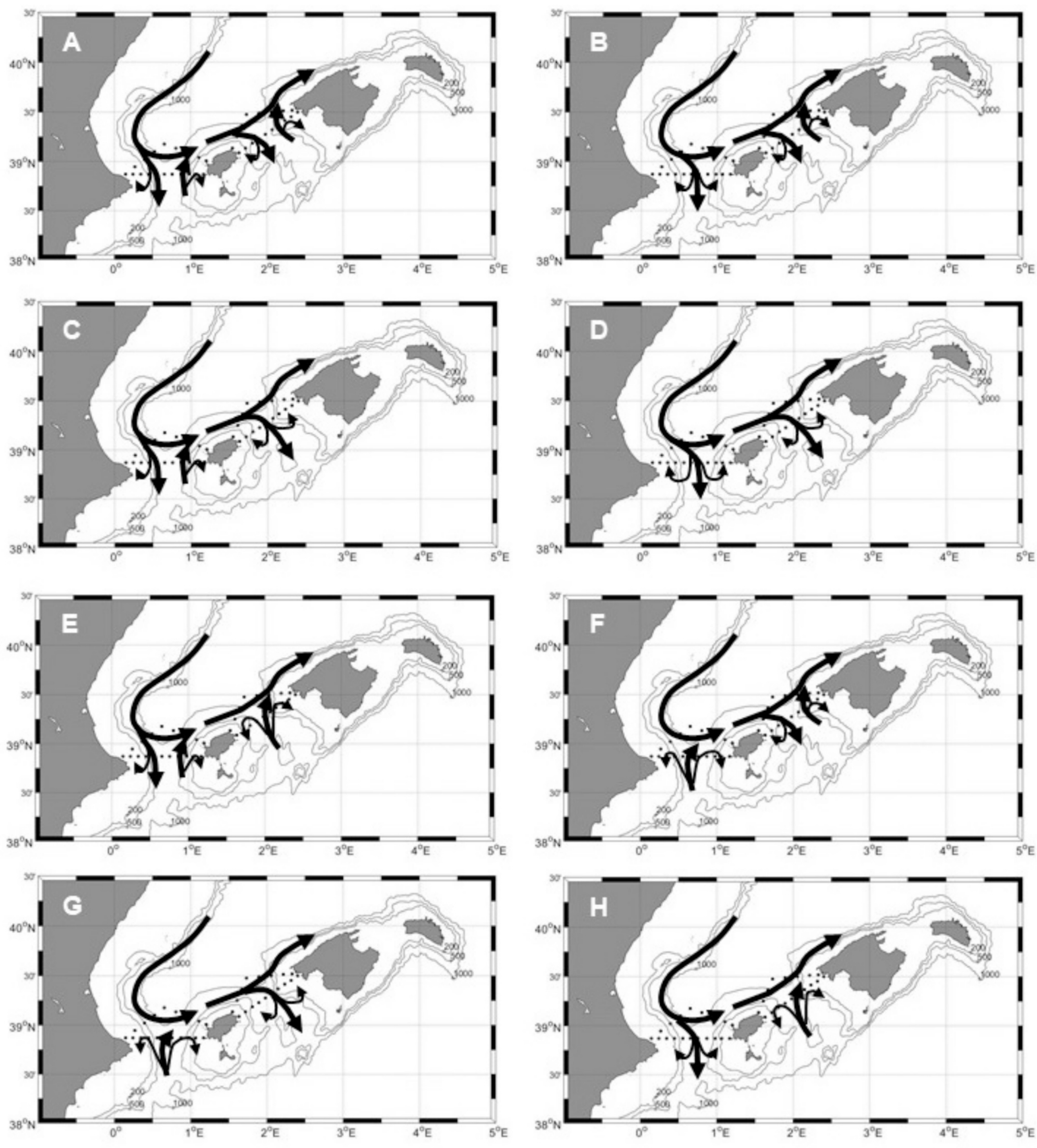

Fig. 11. Plausible schemes of circulation in the Balearic Channels and to the north of the islands inferred from the observed circulation modes at the southern sections of the Channels.

Beside this, let us consider that when the circulation follows the Northern Current mode, it is more intense at the western side and when it follows the inflow mode, it is more intense at the eastern side. In this situation the mean transports would be directed southwards at the western section and northwards at the eastern one. Hence we could infer, from the calculation of the mean transports that the prevailing circulation is a two-way circulation mode when this circulation pattern had never been observed because of the bimodal character of the circulation. This does not imply that the calculation of transports has no importance. On the contrary, the mean transports are needed in order to understand the mass, heat and salt budgets of the Northwestern Mediterranean as well as of any other region of the world oceans. However, understanding the circulation of the channels requires a more detailed analysis as the one proposed in section 3.3 and summarized in Fig. 10. It should be noticed that the classification of the circulation for each campaign has been done in a subjective way. This could be considered a shortcoming of the present work and an objective method for establishing this classification should be developed in the future. Nevertheless, the present study shows the existence of different circulation patterns similar to those described in Barceló-Llull et al. (2019) and in Heslop et al. (2012) and two new circulation modes have been identified. These circulation modes can be combined in different ways in the Ibiza and Mallorca Channels. In order to use as many campaigns as possible and get better statistics, they have been inferred just from the southern sections of both channels (using the geostrophic velocities without the use of the inverse method), which makes it difficult to make an accurate description of the circulation in the Channels and to the north of the Islands. However, Fig. 11 shows an attempt to provide a plausible description of such circulation showing the different combinations that have actually been observed: two-way circulation in both channels (Fig. 11A), Northern Current and two-way circulation (11B and 11C), Northern Current in both channels (Fig. 11D), two-way circulation and inflow (Fig. 11E and F) and finally Northern Current and inflow (Fig. 11G and H). Notice that in all the cases the main direction of the flow is indicated by means of thick arrows. These directions allow us to define the different circulation modes. In addition, thin arrows in Fig. 11 have been included to show the usual counter-currents observed in the shelves of the channels flowing in the opposite direction to that of the flow in the central parts of the channels.

The most frequent combination is the existence of a two-way circulation mode in both channels with the southward flow at the western sides, as an extension of the cold and salty waters of the Northern Current, and a northward flow at the eastern sides, with fresher AW reinforcing the North Balearic Current. The reversal of the two-way circulation mode, with the northward current to the west and the southward current to the east is much less frequent, but has been observed in both channels associated to a deepening of the isopycnals in the central part of the channels and could correspond to the presence of anticyclonic gyres blocking the transports through the channels as already observed by Pinot et al. (2002). These circulation patterns are expected to have a seasonal signal, but the number of campaigns per season is still too low to establish statistically significant differences in the frequency of occurrence of these circulation patterns. Notice that there are 11 campaigns for winter, 17 for spring, 6 for summer and 8 for autumn (42 campaigns). This number considerably decreases if we consider only those campaigns when the complete boxes (triangles) are available (23 campaigns).

Concerning the LIW circulation, the mean transports for the complete sections from Table 2c show very low values for the annual mean transport: −0.0375 Sv for the Ibiza Channel and 0.0025 Sv for the Mallorca one. These two values yield a very low value of −0.038 Sv for the LIW transport through the Balearic Channels. If the inverse method is not used, increasing the number of available campaigns, the LIW transport at the Ibiza Channel is −0.018 Sv and that in the Mallorca Channel is 0.003 Sv, with a net southward transport of −0.015 Sv. As in the case of the upper layer, these results can be placed in a broader context. The formation rate of LIW is close to 1 Sv (Lascaratos et al., 1993) and the LIW transport through the Sicily Channel into the WMED is between 0.91 and 1 Sv according to Béranger et al. (2005) and Bethoux (1980). This water mass flows into the Tyrrhenian Sea where it describes a cyclonic circuit. According to Astraldi and Gasparini (1994) the transport of this water mass through the Corsica Channel is negligible and most of this water mass exits the Tyrrhenian Sea at the southern tip of Sardinia and then turns to the north along the western slope of this island to finally join the Northern Current. This circulation scheme is also proposed by Millot and Taupier-Letage (2005). In addition to this path, LIW could also be entrained by anticyclonic Algerian Eddies drifting westwards within the EAG. To our knowledge there are no estimations of the LIW westward transport linked to this latter mechanism, but a large fraction of the LIW entering the WMED could be expected to follow the Northern Current pathway. In that case, the transport of LIW flowing southwards through the Balearic Channel represents a very small fraction of the LIW that flows cyclonically within the Northern Current around the WMED. This would imply that this water mass would mainly flow along the northern slope of the Balearic Islands within the North Balearic Current.

5. Conclusions

The main conclusions are summarized according to the four objectives outlined in the introduction: This study presents the longest available time series of water transport through the Balearic Channels. When considering the complete sections of the Mallorca and Ibiza Channels, the mean transport estimates derived from these time series qualitatively align with those obtained from average temperature and salinity conditions in Vargas-Yáñez et al. (2020). However, there is no quantitative agreement, nor do the results remain consistent when different sub-sections are analysed.

Regarding seasonal and interannual variability, the results show a year-round southward transport dominance in the Ibiza Channel for both the upper layer (AW and WIW) and the LIW. In contrast, northward transport prevails in the Mallorca Channel. Southward transport intensifies during winter and spring, while northward transport peaks in autumn. However, as demonstrated by Barceló-Llull et al. (2019), Juza et al. (2013), and Heslop et al. (2012), there is substantial interannual and high-frequency variability. Consequently, estimating seasonal or even annual mean transports from limited data remains challenging. As more oceanographic campaigns are conducted, these mean transport estimates will better approximate the true values.

Estimating water transport through the Balearic Channels is crucial for closing the mass budget of the Northwestern Mediterranean. Although instantaneous transports can occasionally reach high values (nearly 1 Sv), mean values remain low, at approximately −0.12 Sv for the upper layer (AW + WIW). This finding suggests that closing the mass budget in this region likely requires a southward transport through the Menorca-Sardinia section. Similarly, the mean annual LIW transport is remarkably small (−0.038 Sv), implying that this water mass primarily flows north of the Balearic Islands via the North Balearic Current before turning southward to complete its cyclonic circulation in the Western Mediterranean. This study further demonstrates that when inverse methods are unavailable, using the sea bottom (or a deep reference level such as 800–900 m) as a no-motion layer provides a reasonable approximation for calculating geostrophic velocities in the upper layer. However, this approach proves less suitable for the LIW, which lies closer to the seafloor.

Finally, our results show that it is not suitable to infer the circulation patterns in the Balearic Channels from the mean transports. This task should be addressed by means of a careful examination of each individual campaign. A first, although subjective, attempt to carry out this analysis has been presented. There is a very large variability in the circulation patterns of this region of the WMED. In addition to the three circulation modes already described in previous works (Barceló-Llul et al., 2019; Heslop et al., 2012), we have found two more circulation modes. The first one is a reversed two-way circulation mode with directions of the currents opposite to those previously reported in the two-way circulation mode. This new circulation mode could be associated to the existence of anticyclonic eddies within the channels. These structures had already been described by Pinot et al. (2002) and could be responsible for the blocking of the circulation. The second new circulation mode described in the present work is the existence of multiple eddies within the channels, evidencing the strong mesoscale activity in the Balearic Sea.

Besides the results summarized above, this work has some shortcomings that open new research lines. First, it evidences the necessity for continuing these time series in the Balearic Channels in order to obtain more accurate values for the mean transports through them. Second, it also evidences the need to obtain accurate estimates of transports through the main passages and straits of this region from in situ data. In this regard, the estimation of water mass seasonal and annual fluxes in the Menorca-Sardinia section and in the Corsica Strait are of paramount importance for the understanding of the upper layer circulation. Cross shelf and slope time series from the northern coasts of the Balearic Islands would be needed in order to confirm the circulation pattern proposed for the LIW.

CRediT authorship contribution statement

Manuel Vargas-Yáñez: Writing – original draft, Methodology, Formal analysis, Conceptualization. **Maxandre Ouradou:** Software, Methodology, Conceptualization. **Francina Moya:** Supervision, Investigation. **Enrique Ballesteros:** Investigation. **Cristina Alonso:** Investigation. **Mariano Serra:** Investigation. **Safo Piñeiro:** Investigation. **Vicenç Moltó:** Investigation. **Rocío Santiago:** Investigation. **Rosa Balbín:** Investigation. **Silvia Sánchez-Aguado:** Investigation. **Mª Carmen García-Martínez:** Supervision, Project administration. **Gabriel Jordà:** Writing – review & editing, Investigation. **Alonso Hernández-Guerra:** Writing – review & editing, Software, Methodology.

Declaration of competing interest

The authors declare that they have no known competing financial interests or personal relationships that could have appeared to influence the work reported in this paper.

Appendix A. Supplementary material

Supplementary data to this article can be found online at https://doi.org/10.1016/j.pocean.2025.103525.

Data availability

Data will be made available on request.

References

Astraldi, M., Gasparini, G.-P., 1994. The seasonal characteristics of the circulation in the tyrrhenian sea, in seasonal and interannual variability of the western Mediterranean sea (Ed. P. La Viollette). Coast. Estuar. Stud. 46. https://doi.org/10.1029/CE046p0115.

Barceló-Llull, B., Pascual, A., Ruiz, S., Escudier, R., Torner, M., Tintoré, J., 2019. Temporal and spatial hydrodynamic variability in the Mallorca channel (western Mediterranean Sea) from 8 years of underwater glider data. J. Geophys. Res.: Oceans 124, 2769–2786. https://doi.org/10.1029/2018JC014636.

Béranger, K., Mortier, L., Crépon, M., 2005. Seasonal variability of water transport through the Straits of Gibraltar, Sicily and Corsica, derived from a high-resolution model of the Mediterranean circulation. Prog. Oceanogr. 66, 341–364. https://doi.org/10.1016/j.pocean.2004.07.013.

Bethoux, J.-P., 1980. Mean water fluxes across sections in the Mediterranean Sea evaluated on the basis of water and salt budgets and of observed salinities. Oceanol. Acta 3 (1), 79–88.

Boukthir, M., Barnier, B., 2000. Seasonal and inter-annual variations in the surface freshwater flux in the Mediterranean Sea from the ECMWF re-analysis project. J. Mar. Syst. 24, 343–354. https://doi.org/10.1016/S0924-7963(99)00094-9.

Brett, G.J., Pratt, L.J., Rypina, I.I., Sánchez-Garrido, J.C., 2020. The Western Alboran Gyre: an analysis of its properties and its exchange with surrounding water. J. Phys. Oceanogr. 50, 3379–3402.

Casanova-Masjoan, M., Joyce, T.M., Pérez-Hernández, M.D., Vélez-Belchí, P., Hernández-Guerra, A., 2018. Changes across 66_w, the Caribbean Sea and the Western boundaries of the North Atlantic Subtropical Gyre. Prog. Oceanogr. 168, 296–309. https://doi.org/10.1016/j.pocean.2018.09.013.

Castellón, A., Font, J., García, E., 1990. The Liguro-Provencal-Catalan current (NW Mediterranean) observed by doppler profiling in the Balearic Sea. Sci. Mar. 54 (3), 269–276.

Conan, P., Millot, C., 1995. Variability of the northern current off Marseilles, western Mediterranean-sea, from February to June 1992. Oceanol. Acta 18 (2), 193–205.

Cotroneo, Y., Celentano, P., Aulicino, G., Perilli, A., Olita, A., Falco, P., Sorgente, R., Ribotti, A., Budillon, G., Fusco, G., et al., 2021. Connectivity analysis applied to mesoscale eddies in the Western Mediterranean Basin. Remote Sens. 13, 4228. https://doi.org/10.3390/rs13214228.

Escudier, R., Mourre, B., Juza, M., Tintoré, J., 2016. Subsurface circulation and mesoscale variability in the Algerian subbasin from altimeter-derived eddy trajectories. J. Geophys. Res. Oceans 121, 6310–6322. https://doi.org/10.1002/2016JC011760.

Gomis, D., Ruiz, S., Pedder, M.A., 2001. Diagnostic analysis of the 3D ageostrophic circulation from a multivariate spatial interpolation of CTD and ADCP. Deep-Sea Res. I 48, 269–295. https://doi.org/10.1016/S0967-0637(00)00060-1.

Herrmann, M., Sevault, F., Beuvier, J., Somot, S., 2010. What induced the exceptional 2005 convection event in the northwestern Mediterranean basin? answers from a modeling study. J. Geophys. Res. 115, C12051. https://doi.org/10.1029/2010JC006162.

Hernández-Guerra, A., Talley, L.D., Pelegrí, J.L., Vélez-Belchí, P., Baringer, M.O., Macdonald, A.M., et al., 2019. The upper, deep, abyssal and overturning circulation in the Atlantic Ocean at 30_s in 2003 and 2011. Prog. Oceanogr. 176, 102136. https://doi.org/10.1016/j.pocean.2019.102136.

Hernández-Guerra, A., Espino-Falcón, E., Vélez-Belchí, P., Pérez-Hernández, M.D., Martínez-Marrero, A., Cana, L., 2017. Recirculation of the canary current in fall 2014. J. Mar. Syst. 174, 25–39. https://doi.org/10.1016/j.jmarsys.2017.04.002.

Hernández-Guerra, A., Talley, L.D., 2016. Meridional overturning transports at 30 S in the Indian and Pacific Oceans in 2002-2003 and 2009. Prog. Oceanogr. 146, 89–120. https://doi.org/10.1016/j.pocean.2016.06.005.

Heslop, E., Ruiz, S., Allen, J.T., López-Jurado, J.L., Renault, L., Tintoré, J., 2012. Autonomous underwater gliders monitoring variability at "choke points" in our ocean system: a case study in theWestern Mediterranean Sea. Geophys. Res. Lett. 39, L20604. https://doi.org/10.1029/2012GL053717.

Juza, M., Mourre, B., Lellouche, J.-M., Tonani, M., Tintoré, J., 2015. From basin to sub-basin scale assessment and intercomparison of numerical simulations in the Western Mediterranean Sea. J. Mar. Syst. 149, 36–49. https://doi.org/10.1016/j.jmarsys.2015.04.010.

Juza, M., Renault, L., Ruiz, S., Tintoré, J., 2013. Origin and pathways of intermediate water in the Northewestern Mediterranean Sea using observations and numerical modelling. J. Geophys. Res. Oceans 118, 6621–6633. https://doi.org/10.1002/2013JC009231.

Knoll, M., Borrione, I., Fiekas, H.-V., Funk, A., Hemming, M. P., Kaiser, J., Onken, R., Queste, B., Russo, A., 2017. Hydrography and circulation west of Sardinia in June 2014Ocean Sci., 13, 889–904, doi: 10.5194/os-13-889-2017.

Lascaratos, A., 1993. Estimation of deep and intermediate water mass formation rates in the Mediterranean Sea. Deep-Sea Res. I1 40 (6), 1327–1332.

López-Jurado, J.L., Balbín, R., Amengual, B., Aparicio-González, A., Fernández de Puelles, M.L., et al., 2015. The RADMED monitoring program: towards an ecosystem approach. Ocean Sci. 11, 645–671. https://doi.org/10.5194/osd-12-645-2015.

López-Jurado, J.L., Díaz del Río, G., 1994. Dinámica asociada a las masas de agua en el Canal de Ibiza en noviembre de 1990 y marzo de 1991. Bol. Inst. Esp. Oceanogr. 10 (1), 3–22.

Mallil, K., Testor, P., Bosse, A., et al., 2022. The Levantine Intermediate Water in the Western Mediterranean and its interactions with the Algerian Gyres: insights from 60 years of observation. Ocean Sci. 18, 937–952. https://doi.org/10.5194/os-18-937-2022.

Margirier, F., Testor, P., Heslop, E., Mallil1, K., Bosse, A., Houpert, L., Mortier, L., Bouin, M.-N., Coppola, L., D'Ortenzio, F., Durrieu de Madron, X., Mourre, B., Prieur, L., Raimbault, P., Taillandier, V., 2020. Abrupt warming and salinification of intermediate waters interplays with decline of deep convection in the Northwestern Mediterranean Sea. Nat. Scient. Rep. 10, 20923. https://doi.org/10.1038/s41598-020-77859-5.

Millot, C., Taupier-Letage, I., 2005. Circulation in the Mediterra- nean Sea. In: Saliot, A. (Ed.), The Mediterranean Sea. Hand- Book of Environmental Chemistry. Springer, Berlin, Heidelberg. https://doi.org/10.1007/b107143.

Olita, A., Iermano, I., Fazioli, L., Ribotti, A., Tedesco, C., Pessini, F., Sorgente, R., 2015. Impact of currents on surface flux computations and their feedback on dynamics at regional scales. Ocean Sci. 11, 657–666.

Pedder, M.A., 1993. Interpolation and filtering of spatial observations using succesive corrections and Gaussian filters. Mon. Wea. Rev. 121, 2889–2902.

Pinardi, N., Zavatarelli, M., Adani, M., Coppini, G., Fratianni, C., Oddo, P., Simoncelli, S., Tonani, M., Lyubartsev, V., Dobricic, S., et al., 2015. The Mediterranean Sea large scale low frequency ocean variability from 1987 to 2007: a retrospective analysis. Prog. Oceanogr. 132, 318–332.

Pinot, J.-M., López-Jurado, J.L., Riera, M., 2002. The CANALES experiment (1996-1998). Interannual, seasonal, and mesoscale variability of the circulation in the Balearic Channels. Prog. Oceanogr. 55, 335–370. https://doi.org/10.1016/S0079-6611(02)00139-8.

Pinot, J.M., Ganachaud, A., 1999. The role of winter intermediate waters in spring-summer circulation of the Balearic Sea: 1. hydrography and inverse modeling. J. Geophys. Res. 104, 29843–29864. https://doi.org/10.1029/1999JC900071.

Pinot, J.M., Tintoré, J., Gomis, D., 1995. Quasi-synoptic variability in the Balearic Sea. Deep Sea Res. Part I 41 (5/6), 897–914.

Poulos, S.E., 2023. Water Masses of the Mediterranean Sea and Black Sea: an overview. Water 15, 3194. https://doi.org/10.3390/w15183194.

Puillat, I., Taupier-Letage, I., Millot, C., 2002. Algerian eddies lifetime can near 3 years. J. Mar. Syst. 31, 245–259. https://doi.org/10.1016/S0924-7963(01)00056-2.

Renault, L., Orguz, T., Pascual, A., Tintoré, J., 2012. Surface circulation in the Alborán Sea (Western Mediterranean) inferred from remotely sensed data. J. Geophys. Res. 117, C08009. https://doi.org/10.1029/2011JC007659.

Ribotti, A., Puillat, I., Sorgente, R., Natale, S., 2004. Mesoscale circulation in the surface layer off the southern and western Sardinia Island in 2000–2002. Chem. Ecol. 20 (5), 345–363. https://doi.org/10.1080/02757540410001727963.

Ruiz, S., Font, J., Emelianov, M., et al., 2002. Deep structure of an open-sea eddy in the Algerian Basin. J. Mar. Syst. 33–34, 179–195. https://doi.org/10.1016/S0924-7963(02)00058-1.

Ruiz, S., Gomis, D., Sotillo, M.G., Josey, S.A., 2008. Characterization of surface heat fluxes in the Mediterranean Sea from a 44-year high-resolution atmospheric data set. Global Planet. Change 63, 258–274. https://doi.org/10.1016/j.gloplacha.2007.12.002.

Schroeder, K., Tanhua, T., Chiggiato, J., Velaoras, D., Josey, S.A., García Lafuente, J., Vargas-Yaáñez, M., 2023. The forcings of the Mediterranean Sea and the physical properties of its water masses. In: Schroeder, K., Chiggiato, J. (Eds.), Oceanography of the Mediterranean Sea, an introductory guide. Elsevier, Amsterdam, Netherlands.

Somot, S., Houpert, L., Sevault, F., Testor, P., Bosse, A., Taupier-Letage, I., Bouin, M.-N., Waldman, R., Cassou, C., Sanchez-Gomez, E., Durrieu de Madron, X., Adloff, F., Nabat, P., Herrmann, M., 2018. Characterizing, modelling and understanding the climate variability of the deep water formation in the North-Western Mediterranean Sea. Clim. Dyn. 2018 (51), 1179–1210. https://doi.org/10.1007/s00382-016-3295-0.

Testor, P., Send, U., Gascard, J.-C., et al., 2005. The mean circulation of the southwestern Mediterranean Sea: Algerian gyres. J. Geophys. Res. 110, C11017. https://doi.org/10.1029/2004JC002861.

Thiébaux, H.J., Pedder, M.A., 1987. Spatial objective analysis with applications in atmospheric science. Academic press, London.

Troupin, C., Pascual, A., Ruiz, S., et al., 2019. The AlborEx data set: sampling mesoscale features in the Alboran Sea. Earth Syst. Sci. Data 11, 129–145. https://doi.org/10.5194/essd-11-129-2019.

Vargas-Yáñez, M., Sánchez-Leal, R.F., Alvera-Azcárate, A., Troupin, C., Moya, F., Ballesteros, E., Serra, M., Balbín, R., Moltó, V., García-Martínez, M.C., 2023a. Opportunity observation of an Algerian Eddy to the south of Cape Palos (Southwestern Mediterranean Sea). Sci. Mar. 87 (3), e070. https://doi.org/10.3989/scimar.05333.070.

Vargas-Yáñez, M., Moya, F., Serra, M., Juza, M., Jordà, G., Ballesteros, E., Alonso, C., Pascual, J., Salat, J., Moltó, V., Tel, E., Balbín, R., Santiago, R., Piñeiro, S., García-Martínez, M.C., 2023b. Observations in the Spanish Mediterranean Waters: a review and update of results of 30-Year monitoring. J. Marine Sci. Eng. 11, 1284. https://doi.org/10.3390/jmse11071284.

Vargas-Yáñez, M., Juza, M., García-Martínez, M.C., Moya, F., Balbín, R., Ballesteros, E., Muñoz, M., Tel, E., Pascual, J., Vélez-Belchí, P., Salat, J., 2021. Long-Term changes in the Water Mass Properties in the Balearic Channels over the period 1996–2019. Front. Mar. Sci. 8, 640535. https://doi.org/10.3389/fmars.2021.640535.

Vargas-Yáñez, M., Juza, M., Balbín, R., Velez-Belchí, P., García-Martínez, M.C., Moya, F., Hernández-Guerra, A., 2020. Climatological temperature and salinity properties and associated water mass transports in the Balearic Channels using repeated observations from 1996 to 2019. Front. Mar. Sci. 7, 568602.

Vargas-Yáñez, M., García-Martíneza, M.C., Moya, F., Balbín, R., López-Jurado, J.L., Serra, M., et al., 2017. Updating temperature and salinity mean values and trends in the Western Mediterranean: the RADMED project. Prog. Oceanogr. 157, 27–46. https://doi.org/10.1016/j.pocean.2017.09.004.

Viúdez, A., Tintoré, J., 1995. Time and space variability in the eastern Alboran Sea from March to May 1990. J. Geophys. Res. 100, 8571–8586. https://doi.org/10.1029/94JC03129.

Wunsch, C., 1978. The North Atlantic general'circulation west of 50_W determined by inverse methods. Rev. Geophys. 16, 583–620. https://doi.org/10.1029/rg016i004p00583.

Wunsch, C., 1996. The Ocean Circulation Inverse Problem. Cambridge University Press, New York, NY.

Zar, J.H., 1984. *Biostatistical Analysis*, 2nd ed. Prentice-Hall, Englewood Cliffs, NJ.